Made available through Montana State University's ScholarWorks

Role of Sparsely Glacierized Basins and Groundwater in Semiarid Andes Periglacial Headwaters

Rémi Valois; Gonzalo Navarro; Shelley MacDonell; Solène Buvat; Giulia de Pasquale; Vincent Marc; Marina Gillon; Esteban Saez Robert; Ayon Garcia; Christopher Ulloa; et al.

Accessibility Disclaimer:

For a more accessible version of this document, please submit an accessibility request form through the Montana State University Library website.

Check for updates

Hydrological Processes

WILEY

RESEARCH ARTICLE OPEN ACCESS

Role of Sparsely Glacierized Basins and Groundwater in Semiarid Andes Periglacial Headwaters

Rémi Valois[1] | Gonzalo Navarro[2,3] | Shelley MacDonell[3,4] | Solène Buvat[5] | Giulia de Pasquale[3] | Vincent Marc[1] | Marina Gillon[1] | Esteban Saez Robert[6] | Ayon Garcia[7] | Christopher Ulloa[7] | Julien Dupont[1] | Milanka Babic[1] | Eric Sproles[8] | Jules Burgat[9] | Etienne Bresciani[10]

[1]Avignon Université, INRAE, UMR 1114 EMMAH, Avignon, France | [2]Universidad de La Serena, La Serena, Chile | [3]Centro de Estudios Avanzados en Zonas Áridas—CEAZA, La Serena, Chile | [4]Waterways Centre, University of Canterbury, Christchurch, New Zealand | [5]Université Clermont Auvergne, CNRS, IRD, OPGC, Laboratoire Magmas et Volcans, Clermont-Ferrand, France | [6]Departamento de Ingeniería Estructural y Geotécnica Santiago, Pontificia Universidad Católica de Chile, Chile | [7]Universidad de Atacama, Copiapó, Chile | [8]Geospatial Snow, Water, and Ice Resources Lab, Department of Earth Sciences, Montana State University, Bozeman, Montana, USA | [9]RECOVER, INRAE Aix-Marseille Université, Aix-en-Provence, France | [10]Instituto de Ciencias de la Ingeniería, Universidad de O'higgins, Rancagua, Chile

Correspondence: Rémi Valois (remi.valois@univ-avignon.fr)

Received: 5 June 2024 | **Revised:** 22 September 2025 | **Accepted:** 29 September 2025

Funding: This work was supported by ECOS-ANID Project (210044/C21U02), ANID-CENTROS REGIONALES (R20F0008), ANID/Scholarship Program/Doctorado Nacional (2021-21210918) and Universidad de La Serena.

Keywords: Andes | cryo-hydrogeological systems | environmental tracers | mountain hydrogeology | proglacial aquifer

ABSTRACT

A better understanding of headwater hydrogeology in the semiarid Andes is critical because high-elevation basins are considered water towers for the main valleys, where water demand is over-allocated. While the body of literature generally focuses on the contribution of glaciers to streamflow, there is little information on the contribution of sparsely glacierized basins and the origins and processes of groundwater generation at high elevations. The Corrales catchment in North-Central Chile contains both heavily and sparsely glacierized sub-basins as well as the highest public borehole in the region, making it suitable to fill such scientific gaps. Geophysical surveys and a pumping test were carried out to obtain information on groundwater flows beneath the Tapado terminal rock glacier and a main tributary of the Elqui River. Radioactive and stable isotopes were used to characterise the hydrological connectivity and the origins of water in the headwater basins. Low electromagnetic velocities and resistivities indicate the presence of liquid water beneath the rock glacier, suggesting the upper limit of a proglacial aquifer. The downstream valley aquifer appears transmissive and dominated by old waters (several decades) that are a mix of high-glacierized and sparsely glacierized basins. In addition, stable isotopes reveal distinct signatures for high-glacierized and sparsely glacierized basins, which may be attributed to isotope fractionation. These results suggest that water isotopes can be used to distinguish between waters originating from high-glacierized and sparsely glacierized basins. The study also identifies the presence of old waters in the sparsely glacierized basins, which indicates long-term storage, slow release or slow turnover times. This finding is crucial for understanding the evolution of late-season baseflow and streamflow in the context of climate change. As the contribution of such basins to total streamflow is significant, a better understanding of hydrological processes in sparsely glacierized regions is required.

This is an open access article under the terms of the Creative Commons Attribution License, which permits use, distribution and reproduction in any medium, provided the original work is properly cited.

© 2025 The Author(s). *Hydrological Processes* published by John Wiley & Sons Ltd.

1 | Introduction

Headwaters in the semiarid Chilean Andes are often considered water towers for the downstream socio-economic needs, providing a significant water contribution from the cryosphere (Navarro, MacDonell, et al. 2023). While the annual streamflow volume is mainly driven by the seasonal snowmelt (i.e., snowfall that almost completely melts during the following summer) (e.g., Favier et al. 2009; Ayala et al. 2023), glaciers and rock glaciers are often considered significant sources of water for maintaining baseflow during low-flow periods (Gascoin et al. 2011; Pourrier et al. 2014; Ragettli et al. 2014; Schaffer et al. 2019). Their contribution is crucial considering the high interannual precipitation variability in the region (Valois et al. 2020a), as well as the ongoing decline in annual precipitation, snowpack accumulation and reservoir storage since 2010. These trends are caused by the persistent Megadrought affecting Central Chile (Garreaud et al. 2017, 2020). This megadrought has been the longest dry period over the last several centuries, characterised by pronounced precipitation deficits. Projections of future climate scenarios show a reduced capacity to meet future water demand during the peak irrigation season (from December to March) (Hublart et al. 2013), earlier peak runoff (Yáñez San Francisco et al. 2023) and the loss of permafrost in high catchments. However, the hydrological implications of the changes are poorly understood (Rogger et al. 2017). Consequently, mountain water resources are expected to be severely affected by these trends, threatening not only water storage but also water generation and water routing in their early stages in the headwater catchment areas.

In this context, research in the semiarid Andes have mainly focused on the cryospheric contribution to runoff, focusing on glacier processes and how the accumulation of seasonal snow contributes to the wider catchment runoff (Ayala et al. 2016; Ragettli et al. 2014). Consequently, other hydrological processes and the importance of basins with a low percentage of its total area occupied by (rock) glaciers and perennial snow have been scarcely studied, leaving a knowledge gap regarding groundwater and sparsely glacierized basins (here defined as a basin where glacier and rock glacier area is $<2\%$ of total area). As such, a better understanding of the hydrogeological functioning of Andean headwaters is needed, especially with regard to hydrological connections between different headwaters units, such as connections between glaciers, debris-covered glaciers, rock glaciers, streamflow and groundwater (e.g., Navarro, MacDonell, et al. 2023). Recent research has shown that periglacial groundwater discharge in the Andes can be a significant contributor to streams during the driest months (e.g., Crespo et al. 2020; Reato et al. 2023; Ruiz Pereira et al. 2023). Despite the fact that conceptual models of glacier systems often include a groundwater component with subglacial and proglacial aquifers (Vincent and Hart 2017; Vincent et al. 2019), direct characterizations of the structure and functioning of such aquifers are scarce worldwide. These proglacial aquifers have been observed to be recharged from glacial and snow meltwater, precipitation and frozen-ground sources—all of which vary seasonally and annually (Williams et al. 2006; Ruiz Pereira et al. 2023). However, their potential role in connecting waters from cryosphere reserves to lowlands is still largely unknown. For instance, it has been recognised that glacial meltwater contributes a considerable percentage to the recharge of some springs in the Cascade Mountains (United States), Livingston and Lewis ranges (United States) (Miller et al. 2021), as well as in the Nevado Coporuna (Peruvian Andes) (Olson et al. 2024). However, there remains a poor understanding of groundwater, snowmelt and ice thaw contributions to streamflow from basins with scant to absence of debris-free glacial occupation.

This study focuses on the Corrales catchment, which is located on the headwaters of the Equi River basin, in the semiarid Chilean Andes (30° S), with the goal of characterising the hydrogeological structure (depth and extension) and function of its proglacial aquifer, as well as to better understand the importance of sparsely glacierized basins for supplying water to the main stream in semiarid regions. We address the following research questions: (i) Are groundwater contributions to streamflow and groundwater outflow from the basin significant processes in headwater periglacial basins? (ii) What is the structure and function of headwater aquifers? Are rock glaciers connected to groundwater systems? (iii) How do sparsely glacierized watersheds play a significant role in late-season baseflow? (iv) How effective are isotopes in differentiating ice and seasonal snow contributions in headwater catchments? The abundance of diverse landforms in the different sub-basins that compose the Corrales catchment makes it an ideal site for understanding meltwater sources and pathways, as well as to better assess the role of proglacial aquifers in transferring flows to lowlands in semiarid catchments.

A combination of hydrogeological methods was employed to address these scientific questions. Hydrogeophysical methods coupled with pumping tests and groundwater level monitoring characterise the proglacial aquifer and groundwater flows. At the same time, hydrochemical analyses (radiogenic and stable water isotopes) were employed to gain information on the dynamics of the hydrogeological headwater system. Our results elucidate the dynamics of periglacial groundwater routing and sources in the semiarid Andes and other arid or semiarid regions around the world. These insights hold particular value in regions without well-developed hydrogeological monitoring and where groundwater is a crucial component of the hydrological cycle.

2 | Materials and Methods

2.1 | Study Site

The study focuses on the Corrales catchment, a $79\,km^2$ catchment located in the headwaters of the Elqui River (~30° S; 4000–5500 m asl), in the Chilean Andes (Figure 1b), with tundra climate at high elevation (Sarricolea et al. 2017). Five main sub-basins are identified in this catchment (named B1–B5, Figure 1c), from where streamflow emerges to feed the Colorado River. The latter river supplies the La Laguna reservoir (3130 m asl, $37.8\,Mm^3$), constructed to support water supply for human and industrial use in the region. The Corrales catchment has a 5.5% glacierized area, including only two glaciers ($1.9\,km^2$), 15 rock glaciers ($2.3\,km^2$ total area) and some perennial snow patches (DGA 2022). The geomorphology of the area is dominated by periglacial and proglacial processes and landforms, along with subordinate fluvial processes in the valley bottom

10991085, 2025, 10, Downloaded from https://onlinelibrary.wiley.com/doi/10.1002/hyp.70294 by Montana State University Library, Wiley Online Library on [17/06/2026]. See the Terms and Conditions (https://onlinelibrary.wiley.com/terms-and-conditions) on Wiley Online Library for rules of use; OA articles are governed by the applicable Creative Commons License

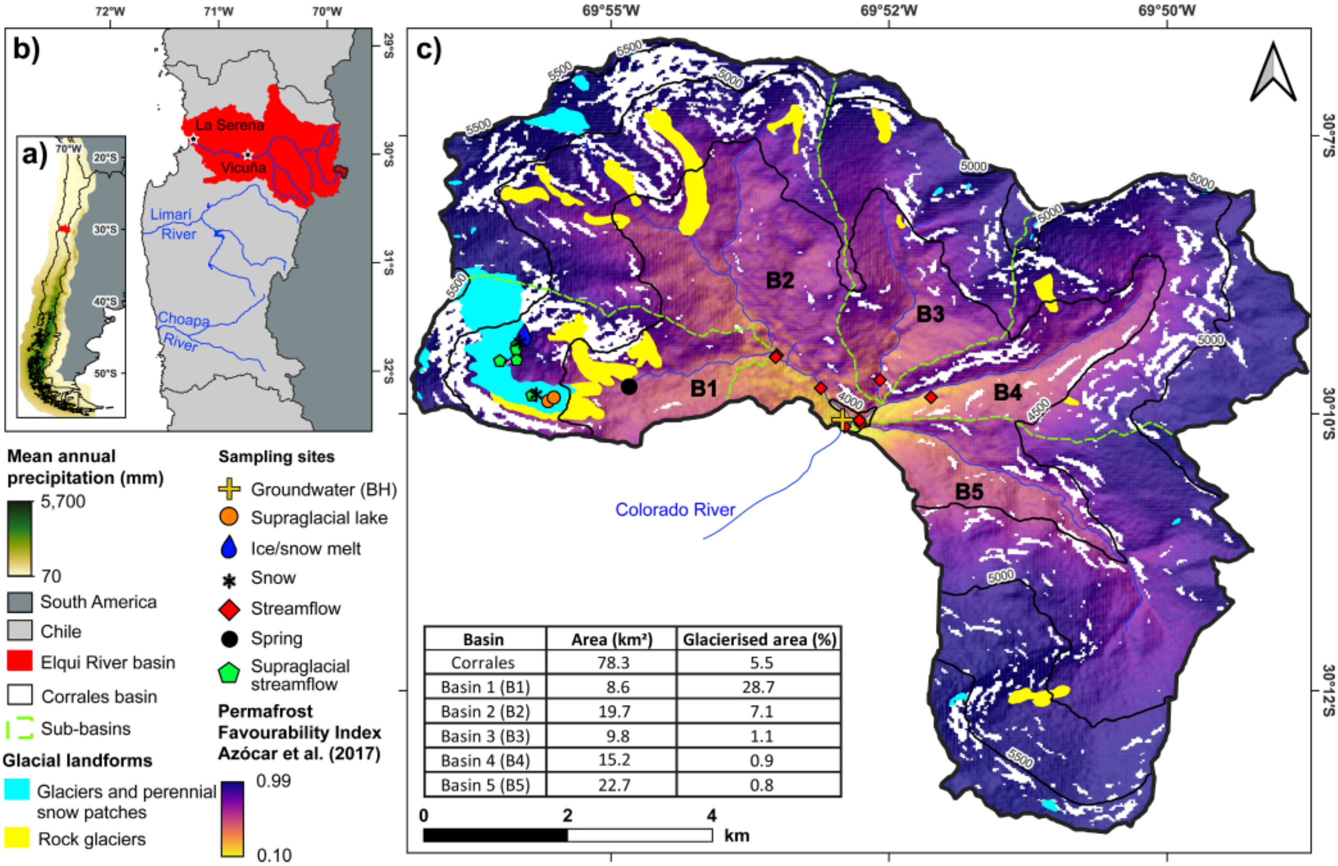

Basin	Area (km²)	Glacierised area (%)
Corrales	78.3	5.5
Basin 1 (B1)	8.6	28.7
Basin 2 (B2)	19.7	7.1
Basin 3 (B3)	9.8	1.1
Basin 4 (B4)	15.2	0.9
Basin 5 (B5)	22.7	0.8

FIGURE 1 | Study location. (a) Annual total precipitation average (mm) between 1979 and 2019, based on the CR2MET high-resolution (0.05° × 0.05°) gridded product v2.5 (Boisier 2023). (b) Location of the Elqui watershed within the Coquimbo region. (c) Location of each water sample on the Corrales basin, showing the Permafrost Favorability Index calculated by Azócar et al. (2017), sub-basins division and cryosphere landforms, according to the national Public Glacier Inventory (Inventario Público de Glaciares; IPG2022v2: DGA 2022).

and gravitational processes in the hillslopes (Velásquez and Natalia 2013). The (peri)glacial landforms are unevenly distributed in the different sub-basins that compose the Corrales catchment. Sub-basin B1 is highly glacierized (28.7%), comprising the Tapado Glacier complex, which features the largest clean-ice glacier in the region. The Tapado Glacier (0.93 km^2 in 2020, Robson et al. 2022) is connected to a debris-covered glacier and rock glaciers (Monnier et al. 2014; Pourrier et al. 2014; Vivero et al. 2021). Sub-basin B2 is the second most glacierized basin (7.1%), which includes a series of rock glaciers and the second clean-ice glacier of the catchment; whereas the three remaining basins (B3–B5) have only a minimal area covered by small (rock) glaciers and perennial snow patches (< 1.1%, Figure 1). There is no evidence of past glaciers in B4 and B5, whereas sub-basin B3 has Pleistocene proglacial moraine deposits (Velásquez Velásquez and Natalia 2013), which could indicate the previous presence of glaciers in the sector.

The Corrales basin has a highly favourable condition for permafrost occurrence above 4500 m asl, as evidenced by the Permafrost Favorability Index (PFI) of Azócar et al. (2017), which shows that 58% of its area has highly favourable conditions for the existence of permafrost (PFI > 0.75) (Figure 1c). Prior research on the rock glaciers in sub-basin B1 reported active layer thicknesses of 4–5 m for the northern Tapado rock glacier (DGA 2022; Milana and Güell 2008; Monnier et al. 2014), with more recent estimates ranging from 3 to 10 m (Navarro, Valois, et al. 2023). The active layer thickness of the nearby rock glacier Las Tolas was determined to be 11 m (Milana and Güell 2008). In Argentina, on the east flank of the Andean Cordillera, at the same latitude, active layer thicknesses have been reported in the order of ~3 m for El Paso rock glacier (Croce and Milana 2002) and of around 3–8 m for Dos Lenguas rock glacier (Halla et al. 2021).

According to Velásquez and Natalia (2013), the area's geology is composed of pyroclastic rocks and breccias, tuffites and subordinate sedimentary rocks. There are also glacial formations with unconsolidated deposits on the proglacial area that are poorly sorted with sub-angular debris.

The annual streamflow volume is mainly derived from the snow cover that almost entirely melts each year (Favier et al. 2009). Precipitation falls predominantly as snow during the winter months and is primarily sourced from humid air masses from the Pacific Ocean (Scaff et al. 2017). The annual mean temperature is about −0.6°C at the Tapado station (4300 m asl). Precipitation shows a very high interannual variability, with annual amounts ranging from less than 20 mm (13 mm in 2019 at the La Serena station at sea level, https://camels.cr2.cl/, last accessed 02 December 2024) to more than 150 mm (177 mm in 2017 at the La Serena station at sea level). Snow sublimation dominates snow dynamics in the region, representing between 30% and 90% of total ablation (Réveillet et al. 2020; Voordendag

10991085, 2025, 10, Downloaded from https://onlinelibrary.wiley.com/doi/10.1002/hyp.70294 by Montana State University Library, Wiley Online Library on [17/06/2026]. See the Terms and Conditions (https://onlinelibrary.wiley.com/terms-and-conditions) on Wiley Online Library for rules of use; OA articles are governed by the applicable Creative Commons License

et al. 2021; Ayala et al. 2023). This process also regulates the occurrence of snowmelt hotspots by reducing the amount of snow available for melting (Ayala et al. 2023). Some summer precipitation occurs, mainly as snowfall, due to local convective thunderstorms as a result of intense surface heating by solar radiation (Aceituno Gutiérrez 1997) or a south-easterly mode of the Bolivian High (Jara et al. 2020). There is, however, a significant runoff contribution from glaciers and rock glaciers during the end of summer and drought periods, supporting baseflow when the snowpack has completely melted (Gascoin et al. 2011; Schaffer et al. 2019).

2.2 | Geophysical Methods

Electrical resistivity tomography (ERT) is a method for estimating the distribution of electrical resistivity in a vertical two-dimensional (2D) cross-section (Dahlin and Zhou 2004). The electrical resistivity provides information on the type of rock, water content and structure. A known electrical current is injected into electrode pairs in an array which diffuses the current underground. Other electrode pairs measure the potential difference, allowing the apparent resistivity to be computed. Inversion of the raw data enables an assessment of the underground resistivity distribution (Loke and Barker 1996).

We performed ERT profiles on the rock glacier area of the Tapado Glacier complex (360 m length) and across the narrow valley (48 m length) at the outlet of the Corrales catchment (Corrales sector, Figure 3a) to gain information on aquifer structure. This method has shown good performance in periglacial environments (de Pasquale et al. 2022; Navarro, Valois, et al. 2023) and in valleys with peatlands (Valois et al. 2020b; Valois et al. 2021) due to the high contrast between saturated and unsaturated sediments and the marked increase in resistivity at the freezing point (Kirsch 2006; Hauck and Kneisel 2008). We employed the Wenner–Schlumberger configuration, using a Syscal Junior switch-48 (IRIS Instruments, France) consisting of two cables using 45 (rock glacier) and 48 (Corrales sector) stainless electrodes (Dahlin and Zhou 2004). The detailed procedure for the rock glacier profile obtained during the 2021 summer is described in Navarro, Valois, et al. (2023). The transect in the Corrales sector of the valley consisted of 48 electrodes spaced 2–5 m apart during the 2019 summer. The Wenner–Schlumberger array was chosen because it provides a good trade-off between sensitivity and signal-to-noise ratio (Valois 2011).

Ground penetrating radar (GPR) has proven to be useful for characterising subsurface characteristics and dynamics associated with freeze–thaw processes and ground ice phenomena in periglacial environments (Annan and Davis 1976). GPR data were collected during the 2021 summer for the rock glacier area using a PulseEKKO PRO DVL system (Sensors & Software Inc., Canada) equipped with bistatic, unshielded antennae operating at 50 MHz. The original GPR dataset was already published in Navarro, Valois, et al. (2023). One common mid-point (CMP) survey was completed on a relatively flat and accessible surface on the rock glacier to assess the electromagnetic velocity distribution with depth. The CMP survey used an initial antenna separation of 2 m, a step size of 0.5 m and a final antenna separation of 41 m (79 traces). The data were processed using EKKO Project v5 (Sensors & Software Inc., Canada). The CMP velocities were interpreted to identify differences in hydrogeological properties with depth, which are dependent on relative water or ice content in the medium (Hauck and Kneisel 2008).

2.3 | Hydrogeological Methods

2.3.1 | Hydrogeological Monitoring

Hydrogeological information at the outlet of the Corrales catchment was derived from the highest public borehole in the region (BH, at approximately 3973 m asl, yellow cross in Figure 1c). The borehole is located 15 m away from the Colorado River, along which peat and grass can grow (Figure 2); such peatlands (or bofedales) are common in the high Andes and constitute biodiversity hotspots (Valois et al. 2021; Navarro, MacDonell, et al. 2023). The well was drilled in February 2016 up to a depth of 30 m without reaching the underlying bedrock. Lithological information is provided in Section 3.1 and Figure 3b. The well has a diameter of 15.24 cm with a screen between 2 and 30 m depth, except from 23 to 25 m to instal a pump. Groundwater level changes were monitored using a CT2X INW vented probe in BH (Figure 2). The hourly record starts in October 2017 and ends in May 2020.

2.3.2 | Pumping Test

We performed a single-well pumping test in the BH during April 2022 to determine the hydraulic properties of the aquifer. The well was pumped for 6 h at a constant rate of 0.7×10^{-3} m^3/s. Water levels were measured manually with an electric dip meter in the pumping well. Measurements were taken at increasing time intervals during both pumping and recovery phases. The recovery phase was monitored over 14 h, at which time the water level returned to its initial level. The pumping test was interpreted using the AQTESOLV software, which incorporates a wide range of analytical solutions (Duffield 2007).

2.3.3 | Discharge Measurements

In addition, salt gauging (Day 1976) was carried out to evaluate streamflow discharge in B1 to B5 basins. This method generally works well in torrential flow conditions (e.g., Valois et al. 2017) such as in the high topographic gradient basins in this study. Discharges were measured in November 2023 and April 2024 at the streamflow sampling sites (Figure 1b).

2.4 | Isotope Sampling and Analysis

Stable isotopes of water (^{18}O, ^{2}H) have been extensively used in mountain hydrology because of the large differences in isotope ratios in rainwater according to altitude. For this reason, they generally provide relevant information on water origin (Poage and Chamberlain 2001; Vitvar et al. 2005; Valois et al. 2021). Tritium is a naturally occurring isotope of hydrogen, formed in the atmosphere primarily through cosmic ray interactions

10991085, 2025, 10, Downloaded from https://onlinelibrary.wiley.com/doi/10.1002/hyp.70294 by Montana State University Library, Wiley Online Library on [17/06/2026]. See the Terms and Conditions (https://onlinelibrary.wiley.com/terms-and-conditions) on Wiley Online Library for rules of use; OA articles are governed by the applicable Creative Commons License

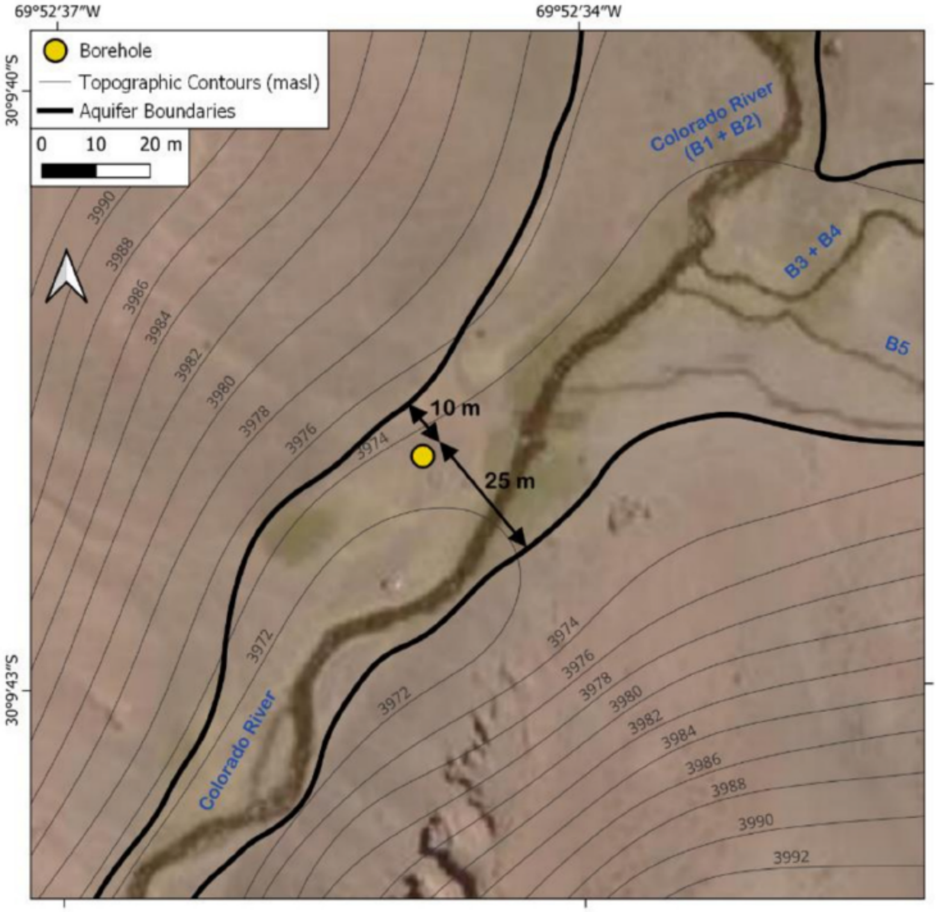

FIGURE 2 | Borehole (BH) location and inferred aquifer boundaries.

or from anthropogenic sources such as nuclear testing. Tritium in precipitation infiltrates into groundwater. As water moves downward through the soil and into deeper aquifers, tritium concentrations decrease, primarily due to mixing with older water and radioactive decay. Thus, tritium (^{3}H) can generally discriminate young waters from older ones due to its relatively fast radioactive decay (Boronina et al. 2005; Eastoe et al. 2012; Stewart and van der Raaij 2022; Desens et al. 2023). However, precipitation tritium activities are approaching levels similar to pre-bomb activities, making it difficult to differentiate modern water from bomb-pulse water (components of 60- to 70-year-old recharge).

In this study, water samples were taken along the different water courses and cryosphere components in the Corrales catchment. Collected waters include snow, snow/ice melt, supraglacial streams, supraglacial lake, groundwater from BH, spring from the Tapado Glacier complex and surface water from each sub-basin and the streams resulting from their junction (eight sites in total). Sampling was performed during four different field campaigns (April 2022, December 2022, March–April 2023, November 2023).

Water was collected in plastic bottles sealed with Parafilm and analysed at the Hydro Lab at Avignon University. Stable water isotope results were normalised to the VSMOW-SLAP scale (Vienna Standard Mean Ocean Water-Standard Light Antarctic Precipitation), using a Picarro L2140-6i spectrometer laser analyzer and they are reported as δ^{18}O and δ^2H in per mil versus VSMOW (‰) for oxygen (^{18}O) and hydrogen (^{2}H) isotopes, respectively, with an analytical error of 0.1‰ for δ^{18}O and 1‰ for δ^2H. Tritium (^{3}H) measurements were performed using a scintillation counter (Tri-Carb 3180 TR/SL) with a detection limit ranging from 0.5 to 0.8 tritium units (TU) and an analytical error ranging from 0.2 to 0.5 TU.

3 | Results

3.1 | Aquifer Structure

The inverted resistivity model (Figure 3c) for the rock glacier on the Tapado Glacier complex shows a shallow sub-horizontal low resistivity zone (< 10 000 Ω m) of ~7–10 m thick overlying a deep high resistive zone (100 000–527 000 Ω m). Such high resistivities were also observed in surrounding rock glaciers (de Pasquale et al. 2022). It is interpreted as the active layer with meltwater above the mixture of ice lenses and rocks. This resistive zone is traversed vertically by an intermediate resistivity zone (between the abscissas 580 and 610 m in Figure 3c), suggesting the presence of vertical pathways of liquid water in the rock glacier. A conductive area was also found beneath the mixture of ice and rocks at the bottom end of the profile, which is interpreted as the presence of liquid water filling the pore space of the debris (Figure 3c). In addition, the CMP result from the GPR survey showed a sharp diminution in

10991085, 2025, 10, Downloaded from https://onlinelibrary.wiley.com/doi/10.1002/hyp.70294 by Montana State University Library, Wiley Online Library on [17/06/2026]. See the Terms and Conditions (https://onlinelibrary.wiley.com/terms-and-conditions) on Wiley Online Library for rules of use; OA articles are governed by the applicable Creative Commons License

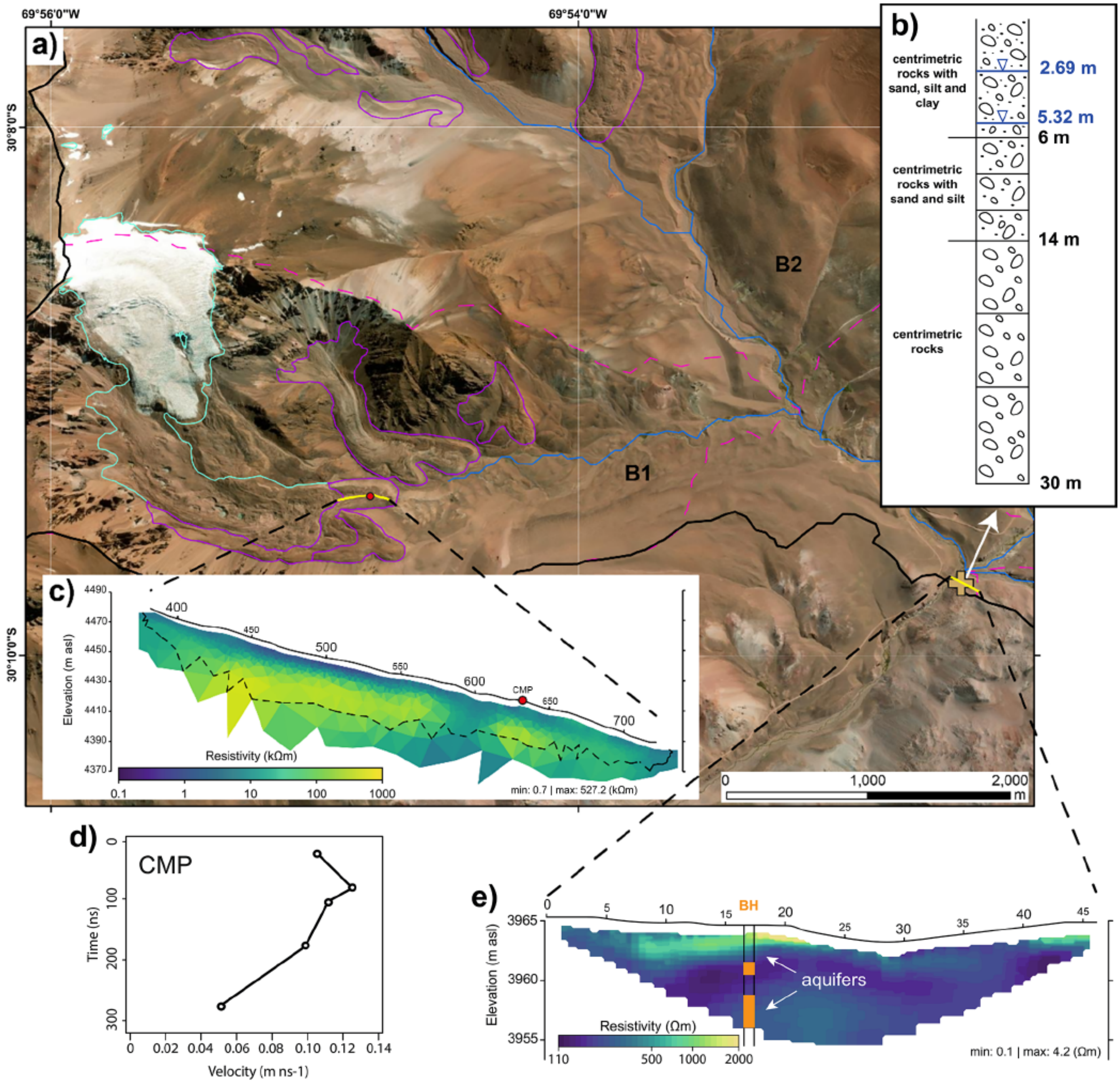

FIGURE 3 | (a) Location of surveys in the western area of the Corrales catchment. (b) Borehole (BH) stratigraphy and groundwater levels. (c) Inverted resistivity tomogram of the rock glacier section (adapted from Navarro, Valois, et al. 2023). (d) Electromagnetic wave velocity analysis from a common mid-point survey on the rock glacier (adapted from Navarro, Valois, et al. 2023). (e) Inverted resistivity tomogram of the downstream valley aquifer (Corrales sector). Yellow lines: ERT transects.

electromagnetic velocity with time (from about 0.11 to 0.05 m/ns, Figure 3d). The time represents the two-way travel time from the antennas to the reflector at depth (Figure A1 presents the original radargram on which hyperbolas were fitted). A longer time equates to a greater depth. Such low values (0.05 m/ns) are indicative of a water-saturated zone, consistent with values reported in the literature (Neal 2004). Thus, both ERT and GPR highlighted the presence of liquid water in the deeper part of the rock glacier, which can cause groundwater flows towards sub or proglacial aquifers. More information on the rock glacier internal structure and its hydrological implications can be found in Navarro, Valois, et al. (2023) and in Pourrier et al. (2014), the latter presenting a comprehensive GPR dataset for the Tapado Glacier.

The lower-elevation ERT cross-section in the narrow valley at the Corrales sector is correlated and calibrated with the information from the borehole stratigraphy recorded during the (air flushing) drilling process. The borehole was drilled up to 30 m depth in glacio-fluvial deposits, without reaching the underlying bedrock. The cuttings showed a heterogeneous granulometry with coarse materials, whereas some fine-grained materials can be found near the surface (Figure 3b). During drilling, a first water level was found at a depth of 2.69 m, while the static

10991085, 2025, 10, Downloaded from https://onlinelibrary.wiley.com/doi/10.1002/hyp.70294 by Montana State University Library, Wiley Online Library on [17/06/2026]. See the Terms and Conditions (https://onlinelibrary.wiley.com/terms-and-conditions) on Wiley Online Library for rules of use; OA articles are governed by the applicable Creative Commons License

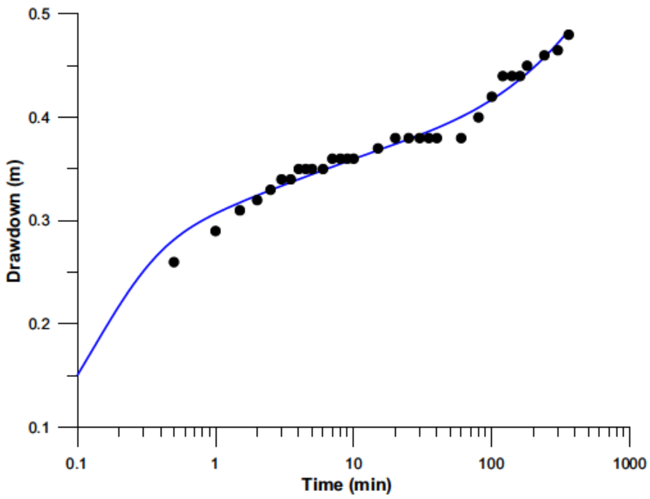

FIGURE 4 | Pumping test data (open circles) and adjusted model (continuous line).

TABLE 1 | Parameter values of the retained pumping test model.

Parameter	Value	CI	Units	Fixed?
r_s	0.0762	NA	m	Yes
r_c	0.0762	NA	m	Yes
r_{eq}	0.02	NA	m	Yes
S_w	0	NA	—	Yes
b	25	NA	m	Yes
T	2.7E−03	[2.23E−03; 2.97E−03]	m^2/s	Variable
K_z/K_r	0.1	[0; 0.19]	—	Variable
S	0.1	[0; 0.45]	—	Variable
S_y	0.226	[0; 0.37]	—	Variable
d	10	NA	m	Yes

Abbreviation: NA, not applicable.

level later stabilised at 5.23 m. This suggests the presence of a shallow aquifer and a deeper aquifer in the coarser material. The shallow aquifer corresponds to the peatland level observed on the site. According to the available lithological information, the deeper aquifer is at least 20-m thick. It is worth noting that a constant downward flow of water occurs through the well, inferred from a significant dripping/flowing noise that can be heard when standing above the borehole. This is interpreted as a consequence of the well connecting the shallow aquifer to the deeper one. The inverted resistivity model for this section shows sub-horizontal resistive zones (300–2000 Ω m) that are well correlated with dry materials near the surface. This is followed at depth by a conductive zone (100–200 Ω m), whose upper part is interpreted as evidence of a thin peatland aquifer, underlain by a clay-rich layer separating the two aquifers. The deeper aquifer is associated with slightly higher resistivities (200–300 Ω m), likely related to a lower silt and clay content relative to the upper layers.

3.2 | Pumping Test and Borehole Monitoring

The drawdown data depict an 'S' shape typical of unconfined aquifer responses on a logarithmic plot (Neuman 1975; Figure 4). While the early phase (where the slope is steeper) may be influenced by wellbore storage (Mucha and Paulikova 1986), wellbore storage alone cannot explain the observed behaviour since the data do not show a unit-slope straight line characteristic of this effect (Bourdet 2002). Hence, it is concluded that the pumped aquifer (i.e., the deeper aquifer, since the water level in the well stands in the deeper aquifer) is unconfined. Equivalently, it is concluded that the shallow aquifer is perched. We discard the impact of the vertical drainage from the shallow aquifer to the pumped aquifer on the time-dependent evolution of drawdown because of: (i) the typical 'S' shape of the unconfined response, (ii) the apparent disconnection between the two aquifers through a rich clay layer, (iii) the significant difference between the pumping rate (0.7 L/s) and the estimated flowrate between the two aquifers inside the borehole (about 0.03 L/s). Nonetheless, we interpreted only the drawdown phase, excluding the recovery, to avoid potential influence from this artificial connection during the aquifer recovery.

Accordingly, the Moench solution (Moench 1997) for pumping in unconfined aquifers was employed to interpret the pumping test. This solution accounts for water release from elastic and phreatic storages, wellbore storage and skin effects. Fixed model parameters include: well outer radius (r_s); well casing radius (r_c); downhole equipment radius (r_{eq}); saturated aquifer thickness (b) (Table 1).

As the pumping well is located in a narrow valley, we included two no-flow boundaries at a 10 and 25 m distance from the well, which is the approximate distance to the closest valley sides where the sediments probably lay against hard rock (Figure 2). Fitting this model yielded as good a match (RMSE = 0.84 cm) and realistic parameter values (Figure 4, Table 1). We did not include any constant-head boundary that would represent the stream, since the groundwater level is several metres below the stream, implying that the stream is disconnected from the aquifer. Based on the above, the Moench model (Moench 1997) with a single no-flow boundary at a 10 m distance was selected to estimate the aquifer parameters (Table 1).

Transmissivity (T) was estimated at $2.7\times10^{-3}\,m^2/s$. Considering the 25 m aquifer thickness, this means $K_r = 1.08\times10^{-4}$ m/s, which is a realistic value for poorly sorted sand (Freeze and Cherry 1979), in agreement with the stratigraphy information (Figure 3b). K_z/K_r was estimated at 0.12, a reasonable value for sedimentary deposits containing clay (Todd and Mays 2004). S and S_y were estimated at 0.1% and 22.6%, respectively, which are within typical ranges of values (Freeze and Cherry 1979). Nonetheless, it is important to note that these estimates are not entirely free of uncertainty. In particular, the 95% confidence interval (CI) calculated as part of the automatic curve fitting in AQTESOLV indicates that only T is well-constrained by the data, whereas the other parameters have more than 100% uncertainty (Table 1). Furthermore, this uncertainty does not account for conceptual uncertainties, and so the true uncertainty is likely larger.

10991085, 2025, 10, Downloaded from https://onlinelibrary.wiley.com/doi/10.1002/hyp.70294 by Montana State University Library, Wiley Online Library on [17/06/2026]. See the Terms and Conditions (https://onlinelibrary.wiley.com/terms-and-conditions) on Wiley Online Library for rules of use; OA articles are governed by the applicable Creative Commons License

Groundwater levels were monitored between 2018 and 2022 (Figure A2) without significant annual or seasonal variation (at about 5.3 m below ground level). Such stable groundwater levels suggest that the aquifer delivers more or less the same amount of water all year long downstream, in addition to having little variation in its stored volume.

3.3 | Hydrogeological Functioning Using Isotopes

3.3.1 | Stable Isotopes

The $\delta^{18}O$ values range from −15.6‰ to −21.0‰ (Table 2), whereas $\delta^{2}H$ values range from −115.31‰ to −150.8‰. The lowest values are at the highest elevations, which is consistent with high-elevation precipitation being depleted in heavy isotopes. There are 11 samples from the B1 basin and only one from the other basins, as the B1 basin includes the glacier complex with several distinct water source possibilities, whereas there may be only one or two water emergences from the other basins. In addition to flows from the sub-basins, snow, borehole samples and the outlet of the five basins were sampled.

The local meteoric water line (LMWL) was calculated using 16 isotope samples in 2015 from seven locations from the sea until the upper part of the Elqui river basin (from 185 to 4300 m asl; Figure 5; Valois et al. 2021; Table 3). It matches the global meteoric water line (GMWL; Craig 1961), as well as two local lines in southern areas that include high elevation sampling locations: the Juncal basin from Rodriguez et al. (2016) and the Aconcagua basin from Taucare et al. (2020). The local line of Oyarzún et al. (2014) in the southern low Limari basin is similar to the four previous lines but with a steeper slope (Table 3). The local line of Spangenberg et al. (2007) from southern Chile (not shown here) is below all sampling points and lines. The two lines in the upper group were calculated at the Elqui coast by Squeo et al. (2006) and in the Northern desert of Pampa del Tamarugal by Aravena et al. (1999).

Stable water isotopes of the sparsely glacierized basins streamflow (B3–B5, Figure 5) and the snow samples are aligned with the GMWL or the similar LMWL, whereas samples from the high-glacierized basin (B1) are above the GMWL, except for the two supraglacial lakes samples. This offset from the MWLs can be explained by liquid-ice isotopic fractionation processes and excess in deuterium (Noor et al. 2023), during the slow partial melting of ice. Water from melting ice is depleted in heavy isotopes. This kinetic depletion of heavy water isotopes during ice melt, associated with deuterium excess, results in a shift to the left of the LMWL (Figure 5). This is corroborated by the isotopic signature of the supraglacial lakes, where the in situ snow and ice melted entirely so that there is no fractionation. The second-highest glacierized basin (containing clean-ice glacier and rock glacier) (B2) sample seems to be closer to the samples originated from partial ice and snow melt. Thus, it highlights as well a distinct signature of high-glacierized basins as compared to sparsely glacierized basins. This spatial pattern could be explained, in theory, by a different mixing between air masses from Pacific and Atlantic for example (lower and upper groups in Figure 5). Nonetheless, neither tritium activities can corroborate this hypothesis since there is no ^{3}H spatial pattern, nor the supraglacial lakes values aligned with the MWLs. In addition, we discarded chemical influences from air masses of Andean eastern side in the discussion below. Thus, fractionation is the most relevant process that can explain the observations.

Because there are many sampling locations in the B1 basin, stable isotopes exhibit larger variation than the others where only the basin outlet streamflow was sampled. The borehole isotopes (BH) do not show a significant variation with the sampling date. Nonetheless, their location between the GMWL and the high-glacierized samples (B1 and B2) highlights probable mixing between the sparsely glacierized and high-glacierized basins.

3.3.2 | Radioactive Isotope Analysis

Seasonal snow shows a considerable amount of tritium content (between 6.3 and 8.6 TU, Figure 5), which is the highest value obtained in this study. It corresponds well to values derived from a regional scale analysis of ^{3}H in precipitation by Basaldúa et al. (2022). Liquid water sampled on the glacier shows significant tritium variations in both time and space. While some samples are below the detection limit (< 0.5 or 0.7 TU), others do show some significant tritium amounts (5 TU). It can be easily explained by the glacier contribution. A glacier can store water for decades, centuries or even longer, so that the water sampled in the glacier, streams or boreholes is a mix of older water with more recent ones.

There is a seasonal tritium content variation that seems to be linked to snowmelt and precipitation amount (Figure 6). Tritium activities are the lowest in April 2022 for the glacier flow in B1, the streamflow that collects B1–B5 and the borehole. It corresponds to the end of the melting season when the 2021 snowpack melted entirely. The percentage of melt water is thus low, and stream flow is dominated by water with larger residence time (groundwater or melting ice) and consequently lower ^{3}H than snow. At the beginning of the melting season in December 2022, tritium content is the highest in the three locations. This can be explained by a larger fraction of seasonal snowmelt with higher tritium content in the sampled water. The final sampling period is at the end of the melting season in April 2023, which shows lower tritium content than at the beginning of the melting season. Nonetheless, tritium content is still higher than in April 2022, which can be explained by a larger amount of snowmelt because of the higher 2022 precipitation amount (138 mm) than in 2021 (58 mm).

Waters sampled in B2 and the borehole have a relatively low tritium content (3.4 and 2 TU respectively in March–April 2022). It can be explained by a mix of older, pre-nuclear age water stored in ice and aquifers with more recent water such as seasonal snow. During the same period, B3 and B5 basins have a quite low tritium content (1.5 TU), which was unexpected from basins that do not present evidence of long-term storage, such as ice or slow aquifers (Thiros et al. 2023). If we assume that these waters are not a mixture because there are few glaciers in the catchment, a simple decay model can be applied to assess a mean residence time. Waters with $^{3}H < 1.5$ TU should have been recharged before 1995 according to the

10991085, 2025, 10, Downloaded from https://onlinelibrary.wiley.com/doi/10.1002/hyp.70294 by Montana State University Library, Wiley Online Library on [17/06/2026]. See the Terms and Conditions (https://onlinelibrary.wiley.com/terms-and-conditions) on Wiley Online Library for rules of use; OA articles are governed by the applicable Creative Commons License

TABLE 2 | Water isotopes for each sample.

Code	Description	Lat. (°)	Long. (°)	Elev. (m asl)	Date	$\delta^{18}O$ ‰ SMOW	$\delta^{2}H$‰ SMOW	Tritium activity (TU)
B1	Debrid-free glacier runoff (moraine)	−30.1502	−69.9233	4672	07 Apr 2022	−19.4	−141.1	0
B1	Moraine spring	−30.1556	−69.9078	4068	07 Apr 2022	−16.8	−120.6	2.5
B1	Supraglacial lake	−30.1569	−69.9080	4302	06 Apr 2022	−16.4	−122.2	0
B1	Tapado Glacier complex outflow (moraine)	−30.1556	−69.9078	4068	21 Dec 2022	−19.0	−136.1	4.9
B1	Snowmelt near the glacier	−30.1502	−69.9233	4672	21 Dec 2022	−20.1	−144.3	4.2
B1	Supraglacial flow (ice and snowmelt?)	−30.1523	−69.9236	4702	21 Dec 2022	−21.0	−150.8	5.9
B1	Supraglacial flow draining a lake	−30.1574	−69.9214	4549	21 Dec 2022	−19.0	−138.1	6.0
B1	Supraglacial flow in DCG	−30.1524	−69.9260	4662	22 Mar 2023	−17.7	−127.4	0.5
B1	Tapado Glacier outflow	−30.1508	−69.9236	4650	23 Mar 2023	−18.7	−134.6	0.9
B1	Supraglacial lake	−30.1577	−69.9182	4537	23 Mar 2023	−15.6	−115.3	3.3
B1	Moraine spring	−30.1557	−69.9078	4275	23 Mar 2023	−17.4	−124.3	3.0
B1	Surface runoff coming from Tapado area	−30.1518	−69.8863	4084	21 Mar 2023	−17.4	−125.4	3.8
B2	Surface runoff from a (rock) glacierised basin	−30.1516	−69.8861	4079	21 Mar 2023	−17.7	−129.6	3.4
B3	Surface runoff near Corrales	−30.1551	−69.8713	4043	22 Mar 2023	−18.1	−137.4	1.4
B4	Surface runoff near Corrales	−30.1576	−69.8639	4578	22 Mar 2023	−17.5	−130.6	3.0
B5	Surface runoff near Corrales	−30.1614	−69.8741	3990	13 Apr 2023	−17.9	−133.8	1.5
BH	Borehole in Corrales (Mixing)	−30.1616	−69.8763	3967	07 Apr 2022	−17.8	−131.3	1.2
BH	Borehole in Corrales (shallow aquifer)	−30.1616	−69.8763	3967	18 Jan 2023	−17.7	−130.4	2.5
BH	Borehole in Corrales (deep aquifer)	−30.1616	−69.8763	3967	13 Apr 2023	−17.7	−131.0	2.0
B1–5 outlet	River water in Corrales	−30.1618	−69.8764	3965	07 Apr 2022	−17.3	−127.4	2.0
	River water in Corrales	−30.1618	−69.8764	3965	21 Dec 2022	−18.1	−130.7	4.4
	River water in Corrales	−30.1618	−69.8764	3965	13 Apr 2023	−17.7	−130.3	2.7

(Continues)

10991085, 2025, 10, Downloaded from https://onlinelibrary.wiley.com/doi/10.1002/hyp.70294 by Montana State University Library, Wiley Online Library on [17/06/2026]. See the Terms and Conditions (https://onlinelibrary.wiley.com/terms-and-conditions) on Wiley Online Library for rules of use; OA articles are governed by the applicable Creative Commons License

TABLE 2 | (Continued)

Code	Description	Lat. (°)	Long. (°)	Elev. (m asl)	Date	$\delta^{18}O$ ‰ SMOW	$\delta^{2}H$‰ SMOW	Tritium activity (TU)
B1 Snow	Snow near the Glacier	−30.1502	−69.9233	4672	21 Dec 2022	−17.4	−132.1	8.6
B1 Snow	Snow	−30.1576	−69.9210	4547	21 Dec 2022	−17.0	−127.4	6.3

Note: Colours refer to basin or type of water.

isotopic composition of precipitation in Basaldúa et al. (2022). Tritium-depleted samples ($^{3}H < 0.5$ TU) are a good indicator of relatively old water and likely contain some component of pre-bomb recharge.

3.4 | Discharge Results

Discharge during the snowmelt season (November) was generally lower than at the end of the summer season (Table 4). Such a result can be explained by a low amount of snowfall in 2023 (Figure 6) as compared to the average. Snowmelt discharge in November 2023 is therefore lower than melt from glaciers in April 2024, as observed in B1 and B2. The sparsely glacierized basins (B3–B5) show less absolute discharge variation between the two surveys, but they contribute 20%–30% of the total streamflow.

Since we observed that B3–B5 are dominated by old water, which possibly originated from active layer thaw, glaciarets or groundwater, we normalised discharge by the sub-basin area (Table 4). B3 shows a similar basin-normalised discharge to B1 and B2 in November 2023, whereas B4 and B5 have lower values that could be caused by underground pathways or less ice melt. In April 2024, there is a clear correlation between the normalised discharge and the relative glacier cover area (Figure 7a), that is, a higher glacier surface area cover corresponds to higher late-summer season discharge.

After April 2024, ice melt can explain the rise (two to five times) of B1 and B2 basin-normalised discharge (Figure 7b), while it is more challenging to identify a comparable process for a similar increase in B4 basin-normalised discharges given its sparsely glacierized area (outlier in Figure 7b). Comparatively, B3 and B5 display a low decrease in basin-normalised discharges between the two gauging periods, which can be explained by a lower snow contribution at the end of the melt season (April) than at its beginning (November). There is also a clear correlation between discharge ratio and glacier relative cover area (Figure 7b), that is, higher glaciated area relates to a higher spring/autumn discharge ratio because of the increasing ice-melt contribution.

4 | Discussion

4.1 | On the Atlantic Source Precipitation

Precipitation from humid air masses could have a distinct origin: from the Pacific or the Atlantic. According to Aravena et al. (1999), the $\delta^{18}O$-depleted measurements observed in the high-altitude Altiplano were associated with processes that impact the air masses that (i) come from the Atlantic Ocean, (ii) travel through the Amazon watershed, (iii) ascend the Andes and (iv) precipitate in the Altiplano. Even if the humid air masses have a distinct stable isotope signature, Magaritz et al. (1989) showed that the isotopic pattern of the springs in the high Andes of northern Chile is mainly a reflection of the altitude of their recharge areas. In addition, Hoke et al. (2013) indicated that precipitation on the eastern slopes of the Andes at ~33° S, at elevations above 2000 m, is largely derived from a westerly, Pacific-source component. For Tapado Glacier, Sinclair and MacDonell (2016) also showed the dominance of Pacific-source precipitation and its impact on isotope signatures in accumulated snow. Air masses from the Atlantic source are expected during the Austral summer. Only 10% of the precipitation amount falls in summer at the La Laguna station between 1964 and 2024. For these reasons, we choose to neglect its effects on isotopes composition, even though humid air masses from the Atlantic are not expected to be significantly different in Pacific-source tritium activity or unaligned with the GWML.

4.2 | On the Role of Sparsely Glacierized Basins

While highly glacierized basins, such as Tapado, provide a substantial portion of the Colorado River discharge, contributing approximately 10% in February 2011 (Pourrier et al. 2014), there is limited information on the contribution of sparsely glacierized sub-basins. The sparsely glacierized sub-basins (B3–B5) exhibit a significant discharge (Table 4) compared to the catchment outlet, highlighting substantial flows from sparsely glacierized areas at the basin scale. The normalised discharge per glacier and rock glaciers areas of B3 and B4 (Table 4; Figure 8) is much higher than B1, B2 or B5, which suggests significant hidden ice reserves or groundwater flow towards the stream. The normalised discharge of B5 is more or less the same as B1 or B2, which could indicate that there are no hidden ice reserves or less groundwater flow contributing to runoff. In addition, those basins (B3, B4, B5) are associated with relatively low tritium values (Figure 8), which indicates that a proportion of those waters were recharged decades ago (Basaldúa et al. 2022; Ruiz Pereira et al. 2023). Snow samples (5.3–8.6 TU) are in agreement with the precipitation tritium measured in Basaldúa et al. (2022) and Ruiz Pereira et al. (2023) (7.1 in the first study, 4.51 and 8.21 TU in the second one, respectively). Thus, it appears that these sparsely glacierized basins are not only impacted by the seasonal snowmelt but also by older waters. While inter-basin flow from the glacierized basins (B1 and B2) seems possible, stable isotopes samples do not support this hypothesis. Stable

10991085, 2025, 10, Downloaded from https://onlinelibrary.wiley.com/doi/10.1002/hyp.70294 by Montana State University Library, Wiley Online Library on [17/06/2026]. See the Terms and Conditions (https://onlinelibrary.wiley.com/terms-and-conditions) on Wiley Online Library for rules of use; OA articles are governed by the applicable Creative Commons License

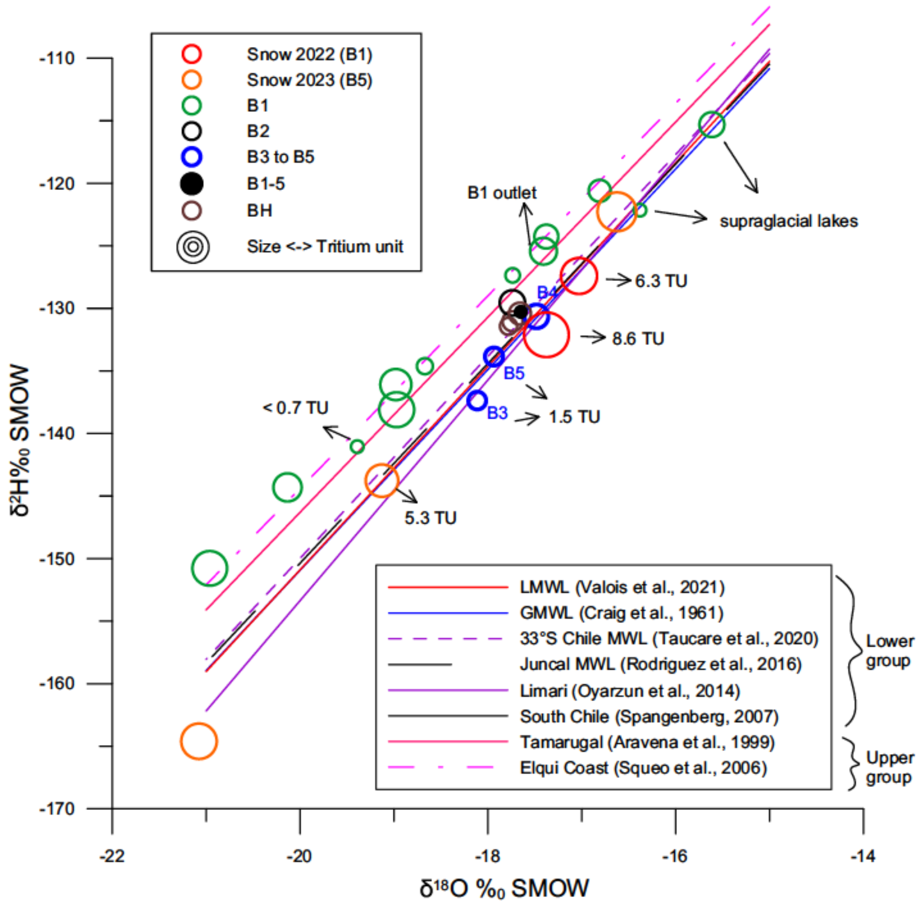

FIGURE 5 | Stable isotopes together with tritium concentration. Circle size is proportional to tritium activity. B1–B5 outlets correspond to streamflow and BH to groundwater.

TABLE 3 | Meteoric water lines.

References	Meteoric lines
Valois et al. (2021)	$8.13\times\delta^{18}O$ ‰ $+ 11.7$
Craig (1961)	$8\times\delta^{18}O$ ‰ $+ 10$
Taucare et al. (2020)	$8.07\times\delta^{18}O$ ‰ $+ 11.42$
Rodriguez et al. (2016)	$7.98\times\delta^{18}O$ ‰ $+ 9.23$
Oyarzún et al. (2014)	$8.8\times\delta^{18}O$ ‰ $+ 23$
Spangenberg et al. (2007)	$8.3\times\delta^{18}O$ ‰ $+ 9.8$
Aravena et al. (1999)	$7.8\times\delta^{18}O$ ‰ $+ 9.7$
Squeo et al. (2006)	$7.7\times\delta^{18}O$ ‰ $+ 9.6$

isotopes from B3 to B5 are indeed aligned with the GMWL (Figure 5), whereas those from B1 to B2 are higher. Thus, the older water presence may be explained by other processes such as storage in aquifers or permafrost thawing.

Talus slope permafrost or hard rock aquifers can indeed act as buffers that delay water flows downstream. Because of past glacial processes and steep topography, Andean headwater basins are often characterised by large amounts of sediments, such as talus slopes and various types of tills. These landforms influence runoff generation because of their buffering capacity (Clow et al. 2003; Liu et al. 2004; McClymont et al. 2010). Snowmelt flows through the subsurface before entering a stream (Campbell et al. 1995; Sueker et al. 2000). In that case, permafrost processes (such as active layer development) may indeed influence storage and subsurface pathways and consequently the basin streamflow response (Koch et al. 2013), with rock glaciers playing a key role in enhancing vertical water pathways (Navarro, Valois, et al. 2023).

Hard rock aquifers in fissured or fractured media can also explain slow water circulation, which induces low tritium activities, as observed in Thiros et al. (2023). In this case, fractured bedrock hosts groundwater with a mixture of residence times ranging from decades to millennia. Other tracers such as ^4He, CFC-12 and SF_6 could allow a robust quantitative estimate of residence times.

The sparsely glacierized basins play a significant role in maintaining interannual baseflow levels with little seasonal snowmelt contribution. It means that there are unknown reserves that must be assessed to predict streamflow evolution under climate change. Thus, studies that aim at better understanding headwaters hydrology or predicting streamflow should include not only highly glacierized basins, but also basins that do not include large, debris-free glaciers, as proposed by Pourrier et al. (2014).

10991085, 2025, 10, Downloaded from https://onlinelibrary.wiley.com/doi/10.1002/hyp.70294 by Montana State University Library, Wiley Online Library on [17/06/2026]. See the Terms and Conditions (https://onlinelibrary.wiley.com/terms-and-conditions) on Wiley Online Library for rules of use; OA articles are governed by the applicable Creative Commons License

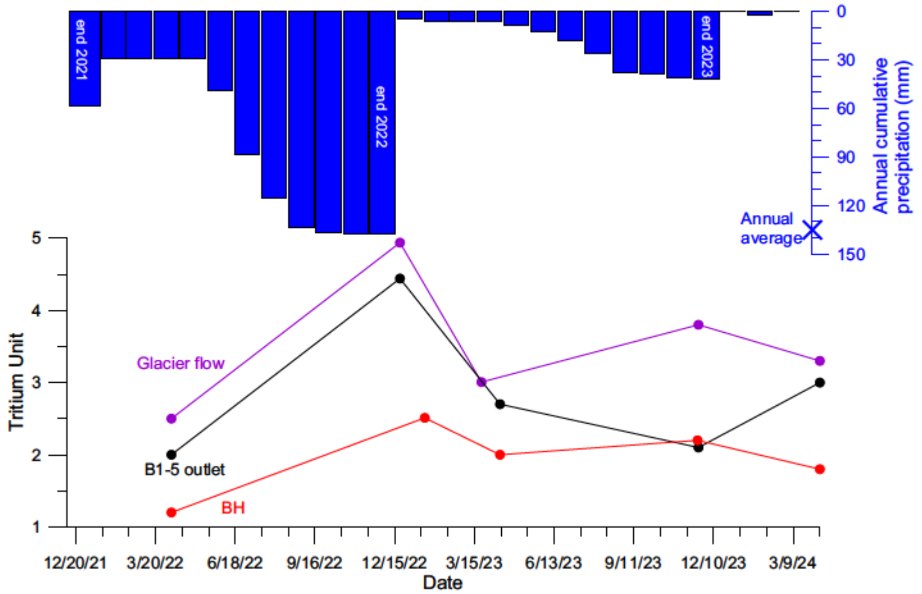

FIGURE 6 | Annual cumulative precipitation at La Laguna station (upper part) together with tritium seasonal variation (lower part). B1–B5 outlets correspond to streamflow and BH to groundwater.

TABLE 4 | Discharge measurements at the outlets of the sub-basins and basin. The results are normalised by the surface areas of sub-basins and by glaciers (G) and rock glaciers (RG) areas.

	Nov 2023		Apr 2024				
	L/s	Per basin area (L/s/km²)	L/s	Per basin area (L/s/km²)	Per G and RG area (L/s/km²)	Ratio 2024/2023	% Ice
B1	14.1	1.64	68.6	7.97	28	4.87	28.7
B2	28.7	1.45	63.3	3.21	45	2.21	7.1
B3	14.4	1.47	11.7	1.19	110	0.81	1.1
B4	5.4	0.36	15.2	1.00	111	2.81	0.9
B5	10.7	0.47	8.2	0.36	45	0.77	0.8
B1–B5	*106.7*	*1.40*	*172*	*2.26*		*1.61*	*5.66*

4.3 | On the Role of Aquifers in Mountainous Periglacial Headwaters

Geophysics revealed the presence of liquid water beneath the terminus of the Tapado rock glacier in sub-basin B1 (Figure 3), such as in the conceptual model of Tapado Glacier of Pourrier et al. (2014). In that study, the glacial foreland was shown to act as a reservoir, storing water during high melt periods and supplying water to downstream compartments during low melt periods. Such water is likely connected to a subglacial or proglacial aquifer that drains the water which percolates to the deeper part of the rock glacier (Figure 8). This aquifer may be connected to lower aquifers, such as in the downstream valley. Geophysical surveys, not presented in this study, used ERT and Time-Domain Electromagnetics (Temfast) to detect groundwater pathways between the proglacial part and the main valley by targeting water content, which corresponds to relatively higher conductivity. However, the conductive volcanic rocks of the study area limit meaningful hydrogeological interpretation. Although groundwater discharge is very difficult to assess in such an environment, efforts should be made, as this hidden discharge may be on the same order as surface flow (Jones 1953; Vincent and Hart 2017) originating from the glacier.

In the lower part of the headwater basins, the borehole intercepts a perched aquifer in the peatland and an unconfined aquifer beneath it made of fluvioglacial deposits. Assuming a hydraulic gradient equal to the topographic gradient (4%) to get a rough estimate of the longitudinal flow of groundwater along the valley from Darcy's law (using the estimated transmissivity of $2.7 \times 10^{-3}\,m^2/s$, aquifer width of 35 m), groundwater flow in the Corrales sector would be equal to 3.8 L/s, that is, about 3.5% of surface water flow at the same location in November 2023. Although this is nearly two orders of magnitude smaller than surface flow, groundwater flow is likely to be constant throughout the year, as indicated by the consistent groundwater levels (Figure A2). In addition, groundwater flows may not be limited by the arbitrary aquifer width and thickness defined here. Deeper and lateral pathways in hard rock aquifers could, of

10991085, 2025, 10, Downloaded from https://onlinelibrary.wiley.com/doi/10.1002/hyp.70294 by Montana State University Library, Wiley Online Library on [17/06/2026]. See the Terms and Conditions (https://onlinelibrary.wiley.com/terms-and-conditions) on Wiley Online Library for rules of use; OA articles are governed by the applicable Creative Commons License

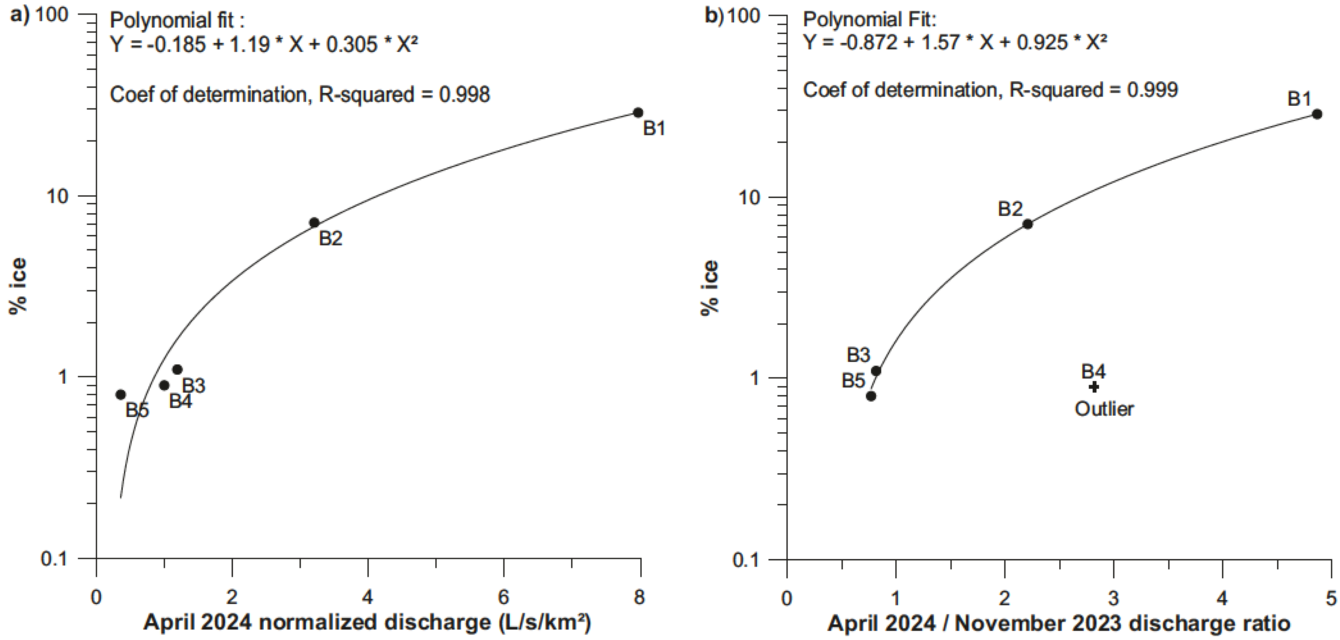

FIGURE 7 | (a) April 2024 discharge and (b) 2024/2023 discharge ratio in function of the relative area covered by glaciers, glaciarets and perennial snow patches.

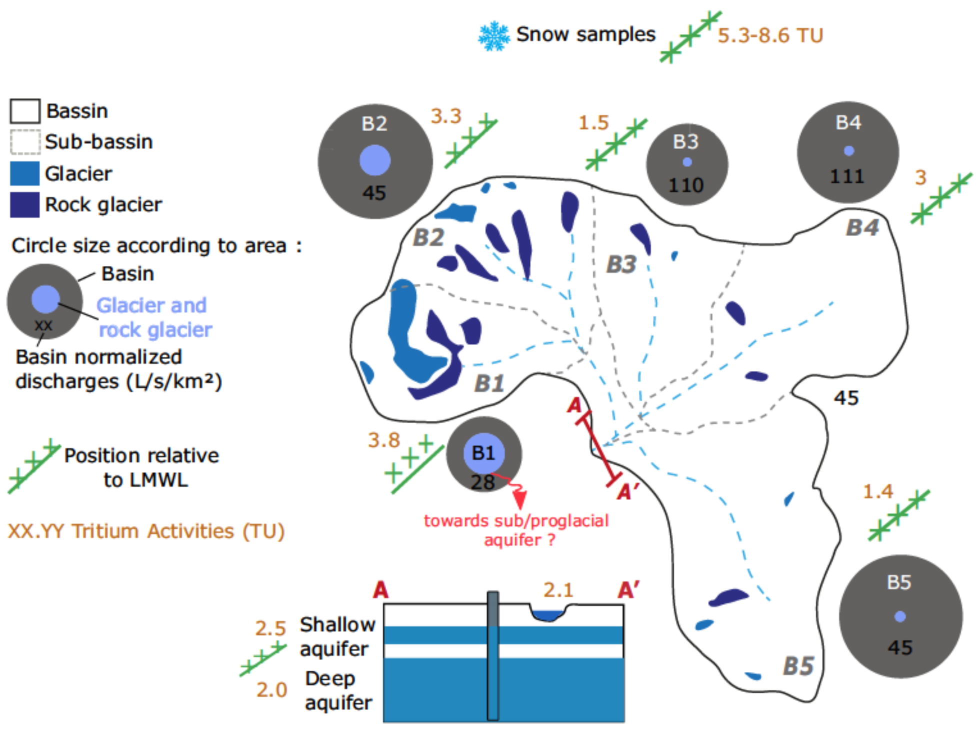

FIGURE 8 | Schematic diagram of the hydrogeological functioning. The snowflake represents snow isotopes signatures. The dark circles areas represent the area of the five basins. The blue circles represent glacierized areas. Black numbers are the basin-normalised discharges per glacierized covered area in L/s/km^2 from the April 2024 survey. Brown numbers are the tritium content in TU. Green symbols represent the alignment of stable isotopes with respect to the GMWL.

course, increase the groundwater contribution to downstream resources. Some water in all of the tributaries likely originates from groundwater, so the 3.5% alone does not fully capture the total groundwater contribution to water resources. Moreover, this estimate carries significant uncertainty due to underlying assumptions, and is most likely lower than actual groundwater contributions. Thus, further studies are needed to more accurately assess groundwater discharge.

Radioactive isotopes showed that the deeper aquifer does present some seasonal variations, with more recent water at the beginning of the melting season, but with less absolute variation than

10991085, 2025, 10, Downloaded from https://onlinelibrary.wiley.com/doi/10.1002/hyp.70294 by Montana State University Library, Wiley Online Library on [17/06/2026]. See the Terms and Conditions (https://onlinelibrary.wiley.com/terms-and-conditions) on Wiley Online Library for rules of use; OA articles are governed by the applicable Creative Commons License

the surface flows (Figure 6). The groundwater sample with the lowest tritium level (1.2 TU) indicates that some of the water was recharged before 1990. This reveals long-term storage, which can be caused by a combination of permafrost change, glacier and slow groundwater velocity. The stable isotopes at three different periods do not present large variations. The measurements taken at the borehole in the Corrales sector could correspond to a mix of the five sub-basins' outlets. Because of its position slightly away from the GMWL, it could correspond at least to a mix of a high-glacierized basin (B1 or B2) that is significantly different from the GMWL and a sparsely glacierized basin (B3, B4 or B5) that is aligned. The groundwater should be composed of a small portion of seasonal snowmelt that infiltrates rapidly through the ground, with slower flows from glaciers and permafrost meltwater or deeper flow through the basement. Given the relatively small dataset, additional sampling is necessary to more accurately quantify the relative contribution of each end-member. Indeed, monitoring the snow isotopes' content evolution, as well as sampling ice and groundwater upstream (glacial, subglacial and proglacial parts) would allow the characterisation of each end-member isotopic signatures.

The aquifer contributes to downstream flow, either with seepage towards the stream or towards downstream aquifers. There is limited information on headwater aquifers and their ability to buffer flows in a changing climate (Hughes et al. 2011; Foster et al. 2017; Wolf et al. 2023; Halloran et al. 2023). Further information is required to evaluate the groundwater discharge, how it is impacted by a changing climate, and how it impacts downstream hydrology.

5 | Conclusions

Aquifer structures and groundwater flow information were obtained using geophysics and isotopes at the front of the glacier and in the valley that collects all flows from the periglacial area. Evidence of water beneath the deep and terminal sectors of a rock glacier, which may flow towards a proglacial aquifer, was derived from GPR and ERT. The lower valley, which collects fluxes from the five studied sub-basins, is composed of a perched aquifer overlying an unconfined aquifer with fairly high transmissivity, as indicated by the pumping test. The observed seasonal variation in tritium levels of groundwater is correlated with precipitation amounts, suggesting that groundwater is a mixture of relatively old water and more recent inputs (Figure 6).

From a methodological perspective, we demonstrated that GPR can identify subglacial aquifers using a CMP survey. In addition, stable isotopes provided evidence of liquid ice fractionation, as observed in other studies, which can help discriminate water originating from glaciers from that derived from seasonal snow.

Tritium activities in all basins and in the borehole are very low, which indicates that some of the water was recharged decades ago. This indicates long-term storage or slow flows in these headwater basins. While long-term storage makes sense in high-glacierized basins, it is less clear in sparsely glacierized basins. It could be explained by slow, deeper groundwater flows. Another explanation would be a contribution from permafrost thaw, without isotope fractionation, such as in the high-glacierized basins. Both explanations highlight the role of sparsely glacierized basins in providing a significant baseflow that was recharged decades ago. Given the relatively small dataset, further studies with other tracers and additional sampling would better characterise each end-member isotopic signature for quantifying the relative contribution of each component (ice, snow, groundwater). Although highly glacierized basins have been proven to play a significant role in the delivery of water during the late season, further investigations are required to assess the potential contribution of sparsely glacierized basins in providing significant water fluxes during low-flow periods and how this contribution would change in a changing climate.

The processes highlighted in this study: (i) the importance of the sparsely glacierized basins in providing significant water amounts to streamflow at the time of the surveys, (ii) the relatively old water in both groundwater and sparsely glacierized basins, (iii) a distinct stable isotope signature for high-glacierized basins, (iv) the presence of liquid water beneath the rock glacier, can be useful to other studies in similar geographical configurations for better modelling or characterising hydrogeological processes and cryosphere-groundwater interactions. Since headwaters are of primary importance for generating streamflow for downstream uses (Hayashi 2020) and because recent advances suggest that high mountain groundwater may provide some resilience—at least temporarily—to climate-driven glacier and snowpack recession (Somers and McKenzie 2020), a better understanding of groundwater and streamflow dynamics and origin is crucial for present and future ecological and socio-economical needs.

Acknowledgements

The authors would like to thank the CEAZA Glaciology and Hydrogeology group for logistical and fieldwork support. The study was supported by ECOS-ANID Project 210044/C21U02 and ANID-CENTROS REGIONALES R20F0008. Gonzalo Navarro was additionally financially supported by Agencia Nacional de Investigación y Desarrollo (ANID)/Scholarship Program/Doctorado Nacional/2021-21210918 and Universidad de La Serena. The authors also thank anonymous reviewers, especially reviewer no. 1 and 3, who helped improve the paper and the graphical abstract.

Data Availability Statement

The data that support the findings of this study are available from the corresponding author upon reasonable request.

References

Aceituno Gutiérrez, P. 1997. "Aspectos Generales del Clima en el Altiplano Sudamericano."

Annan, A. P., and J. L. Davis. 1976. "Impulse Radar Sounding in Permafrost." *Radio Science* 11, no. 4: 383–394.

Aravena, R., O. Suzuki, H. Pena, A. Grilli, A. Pollastri, and H. Fuenzalida. 1999. "Isotopic Composition and Origin of the Precipitation in Northern Chile." *Applied Geochemistry* 14: 411–422.

Ayala, A., F. Pellicciotti, S. MacDonell, et al. 2016. "Modelling the Hydrological Response of Debris-Free and Debris-Covered Glaciers to Present Climatic Conditions in the Semiarid Andes of Central Chile." *Hydrological Processes* 30, no. 22: 4036–4058.

10991085, 2025, 10, Downloaded from https://onlinelibrary.wiley.com/doi/10.1002/hyp.70294 by Montana State University Library, Wiley Online Library on [17/06/2026]. See the Terms and Conditions (https://onlinelibrary.wiley.com/terms-and-conditions) on Wiley Online Library for rules of use; OA articles are governed by the applicable Creative Commons License

Ayala, Á., S. Schauwecker, and S. MacDonell. 2023. "Spatial Distribution and Controls of Snowmelt Runoff in a Sublimation-Dominated Environment in the Semiarid Andes of Chile." *Hydrology and Earth System Sciences Discussions* 27: 3463–3484.

Azócar, G. F., A. Brenning, and X. Bodin. 2017. "Permafrost Distribution Modelling in the Semi-Arid Chilean Andes." *Cryosphere* 11, no. 2: 877–890.

Basaldúa, A., E. Alcaraz, M. Quiroz-Londoño, et al. 2022. "Reconstruction of the Record of Tritium in Precipitation in the Temperate Zone of South America." *Hydrological Processes* 36, no. 9: e14691.

Boisier, J. P. 2023. CR2MET: A High-Resolution Precipitation and Temperature Dataset for the Period 1960–2021 in Continental Chile. (v2. 5)[Data set]. Zenodo.

Boronina, A., P. Renard, W. Balderer, and W. Stichler. 2005. "Application of Tritium in Precipitation and in Groundwater of the Kouris Catchment (Cyprus) for Description of the Regional Groundwater Flow." *Applied Geochemistry* 20, no. 7: 1292–1308.

Bourdet, D. 2002. *Handbook of Petroleum Exploration and Production: Well Test Analysis: The Use of Advanced Interpretation Models*. Vol. 3. Elsevier Science.

Campbell, D. H., D. W. Clow, G. P. Ingersoll, M. A. Mast, N. E. Spahr, and J. T. Turk. 1995. "Processes Controlling the Chemistry of Two Snowmelt-Dominated Streams in the Rocky Mountains." *Water Resources Research* 35: 2811–2821.

Clow, D. W., L. Schrott, R. Webb, D. H. Campbell, A. Torizzo, and M. Dornblaser. 2003. "Ground Water Occurrence and Contributions to Streamflow in an Alpine Catchment, Colorado Front Range." *Groundwater* 41, no. 7: 937–950.

Craig, H. 1961. "Isotopic Variations in Meteoric Waters." *Science* 133, no. 3465: 1702–1703.

Crespo, S. A., C. Lavergne, F. Fernandoy, A. A. Muñoz, L. Cara, and S. Olfos-Vargas. 2020. "Where Does the Chilean Aconcagua River Come From? Use of Natural Tracers for Water Genesis Characterization in Glacial and Periglacial Environments." *Water* 12, no. 9: 2630.

Croce, F. A., and J. P. Milana. 2002. "Internal Structure and Behaviour of a Rock Glacier in the Arid Andes of Argentina." *Permafrost and Periglacial Processes* 13, no. 4: 289–299.

Dahlin, T., and B. Zhou. 2004. "A Numerical Comparison of 2D Resistivity Imaging With 10 Electrode Arrays." *Geophysical Prospecting* 52, no. 5: 379–398.

Day, T. J. 1976. "On the Precision of Salt Dilution Gauging." *Journal of Hydrology* 31, no. 3–4: 293–306.

de Pasquale, G., R. Valois, N. Schaffer, and S. MacDonell. 2022. "Contrasting Geophysical Signatures of a Relict and an Intact Andean Rock Glacier." *Cryosphere* 16, no. 5: 1579–1596.

Desens, A., G. Houben, J. Sültenfuß, V. Post, and G. Massmann. 2023. "Distribution of Tritium-Helium Groundwater Ages in a Large Cenozoic Sedimentary Basin (North German Plain)." *Hydrogeology Journal* 31, no. 3: 621–640.

Dirección General de Aguas. 2022. Inventario público de glaciares, actualización 2022 versión v2. https://dga.mop.gob.cl/Paginas/InventarioGlaciares.aspx.

Duffield, G. M. 2007. *AQTESOLV for Windows—Version 4.5 User's Guide*. HydroSOLVE, Inc.

Eastoe, C. J., C. J. Watts, M. Ploughe, and W. E. Wright. 2012. "Future Use of Tritium in Mapping Pre-Bomb Groundwater Volumes." *Groundwater* 50, no. 1: 87–93.

Favier, V., M. Falvey, A. Rabatel, E. Praderio, and D. López. 2009. "Interpreting Discrepancies Between Discharge and Precipitation in High-Altitude Area of Chile's Norte Chico Region (26–32°S)." *Water Resources Research* 45, no. 2: W02424. https://doi.org/10.1029/2008WR006802.

Foster, T., N. Brozović, and C. Speir. 2017. "The Buffer Value of Groundwater When Well Yield Is Limited." *Journal of Hydrology* 547: 638–649.

Freeze, R. A., and J. A. Cherry. 1979. *Groundwater*. Prentice-Hall.

Garreaud, R. D., C. Alvarez-Garreton, J. Barichivich, et al. 2017. "The 2010–2015 Megadrought in Central Chile: Impacts on Regional Hydroclimate and Vegetation." *Hydrology and Earth System Sciences* 21, no. 12: 6307–6327.

Garreaud, R. D., J. P. Boisier, R. Rondanelli, A. Montecinos, H. H. Sepúlveda, and D. Veloso-Aguila. 2020. "The Central Chile Mega Drought (2010–2018): A Climate Dynamics Perspective." *International Journal of Climatology* 40, no. 1: 421–439.

Gascoin, S., C. Kinnard, R. Ponce, S. Lhermitte, S. MacDonell, and A. Rabatel. 2011. "Glacier Contribution to Streamflow in Two Headwaters of the Huasco River, Dry Andes of Chile." *Cryosphere* 5, no. 4: 1099–1113.

Halla, C., J. H. Blöthe, C. Tapia Baldis, et al. 2021. "Ice Content and Interannual Water Storage Changes of an Active Rock Glacier in the Dry Andes of Argentina." *Cryosphere* 15: 1187–1213.

Halloran, L. J., J. Millwater, D. Hunkeler, and M. Arnoux. 2023. "Climate Change Impacts on Groundwater Discharge-Dependent Streamflow in an Alpine Headwater Catchment." *Science of the Total Environment* 902: 166009.

Hauck, C., and C. Kneisel. 2008. *Applied Geophysics in Periglacial Environments*. Cambridge University Press.

Hayashi, M. 2020. "Alpine Hydrogeology: The Critical Role of Groundwater in Sourcing the Headwaters of the World." *Groundwater* 58, no. 4: 498–510.

Hoke, G. D., J. N. Aranibar, M. Viale, D. C. Araneo, and C. Llano. 2013. "Seasonal Moisture Sources and the Isotopic Composition of Precipitation, Rivers, and Carbonates Across the Andes at 32.5–35.5 S." *Geochemistry, Geophysics, Geosystems* 14, no. 4: 962–978.

Hublart, P., D. Ruelland, A. Dezetter, and H. Jourde. 2013. "Modeling Current and Future Trends in Water Availability for Agriculture on a Semi-Arid and Mountainous Chilean Catchment." In *Cold and Mountain Region Hydrological Systems Under Climate Change: Towards Improved Projections*, vol. 360, 26–32. IAHS/IAPSO/IASPEI Assembly.

Hughes, C. E., D. I. Cendón, M. P. Johansen, and K. T. Meredith. 2011. "Climate Change and Groundwater." In *Sustaining Groundwater Resources: A Critical Element in the Global Water Crisis*, edited by J. A. A. Jones, 97–117. Springer.

Jara, I. A., A. Maldonado, and M. E. de Porras. 2020. "Late Holocene Dynamics of the South American Summer Monsoon: New Insights From the Andes of Northern Chile (21°S)." *Quaternary Science Reviews* 246: 106533.

Jones, P. H. 1953. "Geology and Ground-Water Conditions in the Lower Valley of the Rio Elqui of Chile." *Economic Geology* 48, no. 6: 457–491.

Kirsch, R., ed. 2006. *Groundwater Geophysics: a Tool for Hydrogeology*. Springer.

Koch, J. C., S. A. Ewing, R. Striegl, and D. M. McKnight. 2013. "Rapid Runoff via Shallow Throughflow and Deeper Preferential Flow in a Boreal Catchment Underlain by Frozen Silt (Alaska, USA)." *Hydrogeology Journal* 21, no. 1: 93–106.

Liu, F., M. W. Williams, and N. Caine. 2004. "Source Waters and Flow Paths in an Alpine Catchment, Colorado Front Range, United States." *Water Resources Research* 40: W09401. https://doi.org/10.1029/2004WR003076.

Loke, M. H., and R. D. Barker. 1996. "Rapid Least-Squares Inversion of Apparent Resistivity Pseudosections by a Quasi-Newton Method." *Geophysical Prospecting* 44, no. 1: 131–152.

10991085, 2025, 10, Downloaded from https://onlinelibrary.wiley.com/doi/10.1002/hyp.70294 by Montana State University Library, Wiley Online Library on [17/06/2026]. See the Terms and Conditions (https://onlinelibrary.wiley.com/terms-and-conditions) on Wiley Online Library for rules of use; OA articles are governed by the applicable Creative Commons License

Magaritz, M., R. Aravena, H. Pena, O. Suzuki, and A. Grilli. 1989. "Water Chemistry and Isotope Study of Streams and Springs in Northern Chile." *Journal of Hydrology* 108: 323–341.

McClymont, A. F., M. Hayashi, L. R. Bentley, D. Muir, and E. Ernst. 2010. "Groundwater Flow and Storage Within an Alpine Meadow-Talus Complex." *Hydrology and Earth System Sciences* 14: 859–872. https://doi.org/10.5194/hess-14-859-2010.

Milana, J. P., and A. Güell. 2008. "Diferencias mecánicas e hídricas del Permafrost en Glaciares de Rocas glacigénicos y criogénicos, Obtenidas de Datos sísmicos en El Tapado, Chile." *Revista de la Asociación Geológica Argentina* 63, no. 3: 310–325.

Miller, J. B., M. D. Frisbee, T. L. Hamilton, and S. K. Murugapiran. 2021. "Recharge From Glacial Meltwater Is Critical for Alpine Springs and Their Microbiomes." *Environmental Research Letters* 16, no. 6: 064012.

Moench, A. F. 1997. "Flow to a Well of Finite Diameter in a Homogeneous, Anisotropic Water Table Aquifer." *Water Resources Research* 33, no. 6: 1397–1407.

Monnier, S., C. Kinnard, A. Surazakov, and W. Bossy. 2014. "Geomorphology, Internal Structure, and Successive Development of a Glacier Foreland in the Semiarid Chilean Andes (Cerro Tapado, Upper Elqui Valley, 30°08′ S., 69°55′ W.)." *Geomorphology* 207: 126–140.

Mucha, I., and E. Paulikova. 1986. "Pumping Test Using Large-Diameter Production and Observation Wells." *Journal of Hydrology* 89: 157–164.

Navarro, G., S. MacDonell, and R. Valois. 2023. "A Conceptual Hydrological Model of Semiarid Andean Headwater Systems in Chile." *Progress in Physical Geography: Earth and Environment* 47, no. 5: 668–686.

Navarro, G., R. Valois, S. MacDonell, G. de Pasquale, and J. P. Díaz. 2023. "Internal Structure and Water Routing of an Ice-Debris Landform Assemblage Using Multiple Geophysical Methods in the Semiarid Andes." *Frontiers in Earth Science* 11: 1102620.

Neal, A. 2004. "Ground-Penetrating Radar and Its Use in Sedimentology: Principles, Problems and Progress." *Earth-Science Reviews* 66, no. 3–4: 261–330.

Neuman, S. P. 1975. "Analysis of Pumping Test Data From Anisotropic Unconfined Aquifers Considering Delayed Gravity Response." *Water Resources Research* 11, no. 2: 329–342.

Noor, K., H. Marttila, B. Klöve, J. M. Welker, and P. Ala-aho. 2023. "The Spatiotemporal Variability of Snowpack and Snowmelt Water ^{18}O and ^{2}H Isotopes in a Subarctic Catchment." *Water Resources Research* 59, no. 1: e2022WR033101.

Olson, E. J., L. R. Welp, M. D. Frisbee, et al. 2024. "Spatially Heterogeneous Discharge of Glacial Meltwater to Drainages Surrounding the Ablating Coropuna Ice Cap, Peruvian Andes." *Hydrological Sciences Journal* 69: 1113–1129.

Oyarzún, R., F. Barrera, P. Salazar, et al. 2014. "Multi-Method Assessment of Connectivity Between Surface Water and Shallow Groundwater: The Case of Limarí River Basin, North-Central Chile." *Hydrogeology Journal* 22, no. 8: 1857–1873.

Poage, M. A., and C. P. Chamberlain. 2001. "Empirical Relationships Between Elevation and the Stable Isotope Composition of Precipitation and Surface Waters: Considerations for Studies of Paleoelevation Change." *American Journal of Science* 301, no. 1: 1–15.

Pourrier, J., H. Jourde, C. Kinnard, S. Gascoin, and S. Monnier. 2014. "Glacier Meltwater Flow Paths and Storage in a Geomorphologically Complex Glacial Foreland: The Case of the Tapado Glacier, Dry Andes of Chile (30°S)." *Journal of Hydrology* 519: 1068–1083.

Ragettli, S., G. Cortés, J. McPhee, and F. Pellicciotti. 2014. "An Evaluation of Approaches for Modelling Hydrological Processes in High-Elevation, Glacierized Andean Watersheds." *Hydrological Processes* 28, no. 23: 5674–5695.

Reato, A., E. Carol, and G. Borzi. 2023. "Hydrochemical and Isotopic Composition of Periglacial Watersheds in Northern Patagonian Andes." *Journal of South American Earth Sciences* 123: 104204.

Réveillet, M., S. MacDonell, S. Gascoin, C. Kinnard, S. Lhermitte, and N. Schaffer. 2020. "Impact of Forcing on Sublimation Simulations for a High Mountain Catchment in the Semiarid Andes." *Cryosphere* 14: 147–163. https://doi.org/10.5194/tc-14-147-2020.

Robson, B. A., S. MacDonell, Á. Ayala, T. Bolch, P. R. Nielsen, and S. Vivero. 2022. "Glacier and Rock Glacier Changes Since the 1950s in the La Laguna Catchment, Chile." *Cryosphere* 16, no. 2: 647–665.

Rodriguez, M., N. Ohlanders, F. Pellicciotti, M. W. Williams, and J. McPhee. 2016. "Estimating Runoff From a Glacierized Catchment Using Natural Tracers in the Semi-Arid Andes Cordillera." *Hydrological Processes* 30, no. 20: 3609–3626.

Rogger, M., G. B. Chirico, H. Hausmann, et al. 2017. "Impact of Mountain Permafrost on Flow Path and Runoff Response in a High Alpine Catchment." *Water Resources Research* 53, no. 2: 1288–1308.

Ruiz Pereira, S., B. Díez, J. Cifuentes-Anticevic, et al. 2023. "Hydrological Connections in a Glaciated Andean Catchment Under Permafrost Conditions (33°S)." *Journal of Hydrology: Regional Studies* 45: 101311.

Sarricolea, P., M. Herrera-Ossandon, and Ó. Meseguer-Ruiz. 2017. "Climatic Regionalisation of Continental Chile." *Journal of Maps* 13, no. 2: 66–73.

Scaff, L., J. A. Rutllant, D. Rahn, S. Gascoin, and R. Rondanelli. 2017. "Meteorological Interpretation of Orographic Precipitation Gradients Along an Andes West Slope Basin at 30°S (Elqui Valley, Chile)." *Journal of Hydrometeorology* 18, no. 3: 713–727.

Schaffer, N., S. MacDonell, M. Réveillet, E. Yáñez, and R. Valois. 2019. "Rock Glaciers as a Water Resource in a Changing Climate in the Semiarid Chilean Andes." *Regional Environmental Change* 19: 1263–1279.

Sinclair, K. E., and S. MacDonell. 2016. "Seasonal Evolution of Penitente Glaciochemistry at Tapado Glacier, Northern Chile." *Hydrological Processes* 30: 176–186. https://doi.org/10.1002/hyp.10531.

Somers, L. D., and J. M. McKenzie. 2020. "A Review of Groundwater in High Mountain Environments." *Wiley Interdisciplinary Reviews: Water* 7, no. 6: e1475.

Spangenberg, J. E., B. Dold, M. L. Vogt, and H. R. Pfeifer. 2007. "Stable Hydrogen and Oxygen Isotope Composition of Waters From Mine Tailings in Different Climatic Environments." *Environmental Science & Technology* 41, no. 6: 1870–1876.

Squeo, F. A., R. Aravena, E. Aguirre, A. Pollastri, C. B. Jorquera, and J. R. Ehleringer. 2006. "Groundwater Dynamics in a Coastal Aquifer in North-Central Chile: Implications for Groundwater Recharge in an Arid Ecosystem." *Journal of Arid Environments* 67, no. 2: 240–254.

Stewart, M. K., and R. W. van der Raaij. 2022. "Response of the Christchurch Groundwater System to Exploitation: Carbon-14 and Tritium Study Revisited." *Science of the Total Environment* 817: 152730.

Sueker, J. K., J. N. Ryan, C. Kendall, and R. D. Jarrett. 2000. "Determination of Hydrological Pathways During Snowmelt for Alpine/Subalpine Basins, Rocky Mountain National Park, Colorado." *Water Resources Research* 36: 63–75.

Taucare, M., L. Daniele, B. Viguier, A. Vallejos, and G. Arancibia. 2020. "Groundwater Resources and Recharge Processes in the Western Andean Front of Central Chile." *Science of the Total Environment* 722: 137824.

Thiros, N. E., E. R. Siirila-Woodburn, P. J. Dennedy-Frank, K. H. Williams, and W. P. Gardner. 2023. "Constraining Bedrock Groundwater Residence Times in a Mountain System With Environmental Tracer Observations and Bayesian Uncertainty Quantification." *Water Resources Research* 59, no. 2: e2022WR033282.

10991085, 2025, 10, Downloaded from https://onlinelibrary.wiley.com/doi/10.1002/hyp.70294 by Montana State University Library, Wiley Online Library on [17/06/2026]. See the Terms and Conditions (https://onlinelibrary.wiley.com/terms-and-conditions) on Wiley Online Library for rules of use; OA articles are governed by the applicable Creative Commons License

Todd, D. K., and L. W. Mays. 2004. *Groundwater Hydrology*. John Wiley & Sons.

Valois, R. 2011. "Caractérisation structurale de morphologies karstiques superficielles et suivi temporel de l'infiltration à l'aide des méthodes électriques et sismiques." Doctoral diss., Université Pierre et Marie Curie-Paris VI.

Valois, R., J. Araya Vargas, S. MacDonell, et al. 2021. "Improving the Underground Structural Characterization and Hydrological Functioning of an Andean Peatland Using Geoelectrics and Water Stable Isotopes in Semi-Arid Chile." *Environmental Earth Sciences* 80: 41.

Valois, R., S. MacDonell, J. H. Núñez Cobo, and H. Maureira-Cortés. 2020b. "Groundwater Level Trends and Recharge Event Characterization Using Historical Observed Data in Semi-Arid Chile." *Hydrological Sciences Journal* 65, no. 4: 597–609.

Valois, R., N. Schaffer, R. Figueroa, et al. 2020a. "Characterizing the Water Storage Capacity and Hydrological Role of Mountain Peatlands in the Arid Andes of North-Central Chile." *Water* 12, no. 4: 1071.

Valois, R., J. M. Vouillamoz, S. Lun, and L. Arnout. 2017. "Assessment of Water Resources to Support the Development of Irrigation in Northwest Cambodia: A Water Budget Approach." *Hydrological Sciences Journal* 62, no. 11: 1840–1855.

Velásquez, P., and F. Natalia. 2013. *Geoquímica de Las Rocas ígneas del Carbonífero-Triásico de la Alta Cordillera*. Región de Atacama.

Vincent, A., and J. Hart. 2017. "Under the Glacier, the Groundwater—The Case of Skálafell Area, Iceland." In *Proceedings of 19th EGU General Assembly, EGU2017*.

Vincent, A., S. Violette, and G. Aðalgeirsdóttir. 2019. "Groundwater in Catchments Headed by Temperate Glaciers: A Review." *Earth-Science Reviews* 188: 59–76.

Vitvar, T., P. K. Aggarwal, and J. J. McDonnell. 2005. "A Review of Isotope Applications in Catchment Hydrology." In *Isotopes in the Water Cycle: Past, Present and Future of a Developing Science*, edited by P. K. Aggarwal, J. R. Gat, and K. F. Froehlich, 151–169. Springer.

Vivero, S., X. Bodin, D. Farías-Barahona, et al. 2021. "Combination of Aerial, Satellite, and UAV Photogrammetry for Quantifying Rock Glacier Kinematics in the Dry Andes of Chile (30°S) Since the 1950s." *Frontiers in Remote Sensing* 2: 784015.

Voordendag, A., M. Réveillet, S. MacDonell, and S. Lhermitte. 2021. "Snow Model Comparison to Simulate Snow Depth Evolution and Sublimation at Point Scale in the Semi-Arid Andes of Chile." *Cryosphere* 15: 4241–4259. https://doi.org/10.5194/tc-2021-9.

Williams, M. W., M. Knauf, N. Caine, F. Liu, and P. L. Verplanck. 2006. "Geochemistry and Source Waters of Rock Glacier Outflow, Colorado Front Range." *Permafrost and Periglacial Processes* 17, no. 1: 13–33.

Wolf, M. A., L. R. Jamison, D. K. Solomon, C. Strong, and P. D. Brooks. 2023. "Multi-Year Controls on Groundwater Storage in Seasonally Snow-Covered Headwater Catchments." *Water Resources Research* 59, no. 6: e2022WR033394.

Yáñez San Francisco, E., J. A. Pascual Aguilar, and S. MacDonell. 2023. "Hydrological Response of a Headwater Catchment in the Semi-Arid Andes (30°S) to Climate Change." *Journal of Water and Climate Change* 14, no. 10: 3617–3634.

10991085, 2025, 10, Downloaded from https://onlinelibrary.wiley.com/doi/10.1002/hyp.70294 by Montana State University Library, Wiley Online Library on [17/06/2026]. See the Terms and Conditions (https://onlinelibrary.wiley.com/terms-and-conditions) on Wiley Online Library for rules of use; OA articles are governed by the applicable Creative Commons License

Appendix A

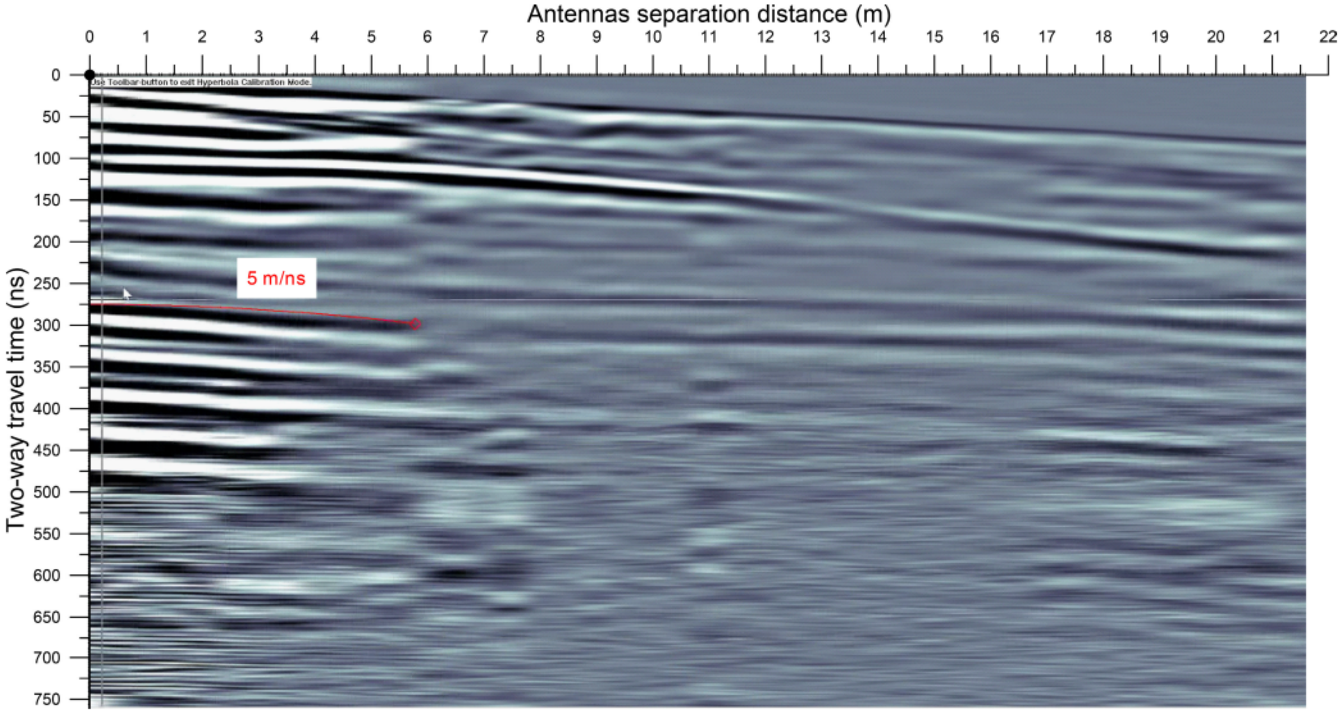

FIGURE A1 | CMP radargram on the rock glacier in B1 basin (Figure 2).

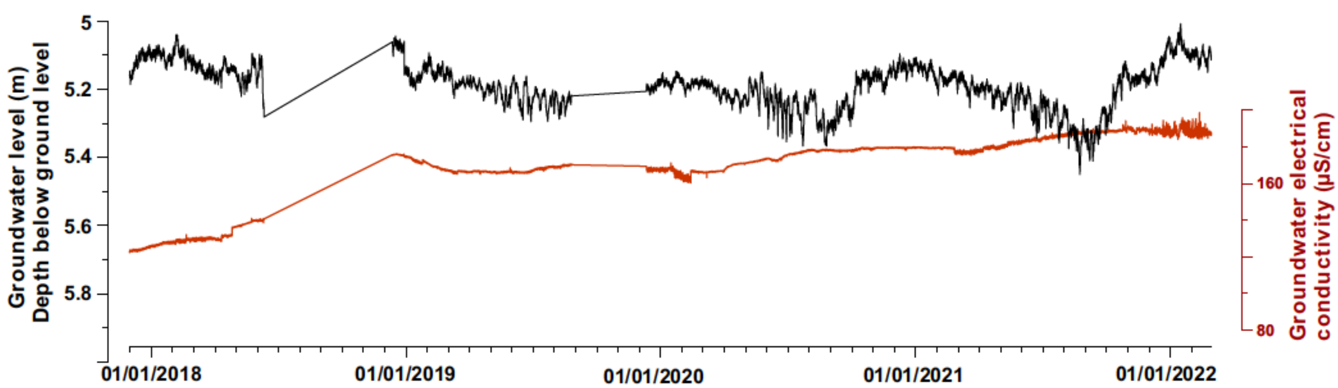

FIGURE A2 | Groundwater level at the Corrales borehole (BH).

10991085, 2025, 10, Downloaded from https://onlinelibrary.wiley.com/doi/10.1002/hyp.70294 by Montana State University Library, Wiley Online Library on [17/06/2026]. See the Terms and Conditions (https://onlinelibrary.wiley.com/terms-and-conditions) on Wiley Online Library for rules of use; OA articles are governed by the applicable Creative Commons License